White Rose Research Online

eprints@whiterose.ac.uk
https://eprints.whiterose.ac.uk
Universities of Leeds, Sheffield and York

Deposited via The University of Leeds.

White Rose Research Online URL for this paper:
https://eprints.whiterose.ac.uk/id/eprint/197901/

Version: Preprint

Preprint:
Sun, K, Muller, M, Macfarlane, C et al. (2023) A novel interaction between the 5' untranslated region of the Chikungunya virus genome and Musashi RNA binding protein is essential for efficient virus genome replication. [Preprint - Cold Spring Harbor Laboratory]

https://doi.org/10.1101/2023.03.29.534719

Reuse
Items deposited in White Rose Research Online are protected by copyright, with all rights reserved unless indicated otherwise. They may be downloaded and/or printed for private study, or other acts as permitted by national copyright laws. The publisher or other rights holders may allow further reproduction and re-use of the full text version. This is indicated by the licence information on the White Rose Research Online record for the item.

Takedown
If you consider content in White Rose Research Online to be in breach of UK law, please notify us by emailing eprints@whiterose.ac.uk including the URL of the record and the reason for the withdrawal request.

UNIVERSITY OF LEEDS
University of Sheffield
UNIVERSITY of York

bioRxiv preprint doi: https://doi.org/10.1101/2023.03.29.534719; this version posted March 29, 2023. The copyright holder for this preprint (which was not certified by peer review) is the author/funder, who has granted bioRxiv a license to display the preprint in perpetuity. It is made available under aCC-BY 4.0 International license.

A novel interaction between the 5' untranslated region of the Chikungunya virus genome and Musashi RNA binding protein is essential for efficient virus genome replication

Authors: Kaiwen Sun, Marietta Müller, Catriona Macfarlane, Mark Harris and Andrew Tuplin*

Correspondence: a.k.tuplin@leeds.ac.uk

Affiliations: Astbury Centre for Structural Molecular Biology and School of Molecular and Cellular Biology, Faculty of Biological Sciences, University of Leeds, Leeds LS2 9JT, UK.

bioRxiv preprint doi: https://doi.org/10.1101/2023.03.29.534719; this version posted March 29, 2023. The copyright holder for this preprint (which was not certified by peer review) is the author/funder, who has granted bioRxiv a license to display the preprint in perpetuity. It is made available under aCC-BY 4.0 International license.

Abstract

Chikungunya virus (CHIKV) is a re-emerging, pathogenic alphavirus that is transmitted to humans by *Aedes spp*. mosquitoes—causing fever and debilitating joint pain, with frequent long-term health implications and high morbidity. The CHIKV lifecycle is poorly understood and specific antiviral therapeutics or vaccines are lacking. In the current study, we identify host cell Musashi RNA binding protein-2 (MSI-2) as a proviral factor. MSI-2 depletion and small molecule inhibition assays, demonstrated that MSI-2 is required for efficient CHIKV genome. Depletion of both MSI-2 and MSI-1 homologues resulted in a synergistic increase in CHIKV inhibition, suggesting redundancy in their proviral function. EMSA competition studies demonstrated that MSI-2 interacts specifically with an RNA binding motif within the 5' untranslated region (5'UTR) of CHIKV and reverse genetic analysis showed that mutation of the binding motif inhibited genome replication and blocked rescue of mutant virus. For the first time, this study identifies the proviral role of MSI RNA binding proteins in the replication of the CHIKV genome, providing important new insight into mechanisms controlling replication of this significant human pathogen and offers the potential of a new therapeutic target.

INTRODUCTION

bioRxiv preprint doi: https://doi.org/10.1101/2023.03.29.534719; this version posted March 29, 2023. The copyright holder for this preprint (which was not certified by peer review) is the author/funder, who has granted bioRxiv a license to display the preprint in perpetuity. It is made available under aCC-BY 4.0 International license.

Chikungunya virus (CHIKV) is an alphavirus of the *Togaviridae* family that is transmitted by *Aedes spp.* mosquitos. CHIKV is closely related to other alphaviruses such as Semliki Forest virus (SFV), Venezuelan equine encephalitis virus (VEEV), and sindbis virus (SINV) [1, 2]. CHIKV was first identified in Tanzania in 1952 and symptoms typically include acute febrile symptoms, myalgia, rash and severe arthralgic joint pain, which may persist for months or years [3]. CHIKV recently caused epidemic outbreaks across regions in Asia, Africa, the Americas, the Middle East and Southern Europe [3]. To date, three phylogenetically distinct lineages of CHIKV have been identified, namely the West African, Asian and the East Central Southern African (ECSA) lineages [4]. There remains no clinically approved vaccine or specific antiviral therapy, due in part to a lack of detailed understanding of the CHIKV replication cycle and its interaction with host cell factors.

CHIKV is an enveloped, positive-sense single-stranded RNA virus with a ~11.8 Kb genome, containing two open reading frames (ORFs) flanked by 5' and 3' untranslated regions (UTRs) (**Fig. 1A**). The 5' UTR is ~ 76 nts in length and is capped by 5' type-0 N-7-methylguanosine. The upstream ORF (ORF-1) encodes the viral non-structural proteins 1-4 (nsP1-4), which are translated directly from the genomic RNA as a single polyprotein that is subsequently proteolytically cleaved into the four mature proteins [5]. Through analogy with other alphaviruses, proteolytic cleavage of nsP1-4 in *cis* by nsP2 releases nsP4 which, as the RNA-dependent RNA polymerase (RdRp), initiates synthesis of the minus-strand intermediate RNA. Subsequent proteolytic cleavage of the remaining nsP123 polyprotein initiates replication of genomic and sub-genomic (29S) RNAs from the minus-strand template [6]. The

bioRxiv preprint doi: https://doi.org/10.1101/2023.03.29.534719; this version posted March 29, 2023. The copyright holder for this preprint (which was not certified by peer review) is the author/funder, who has granted bioRxiv a license to display the preprint in perpetuity. It is made available under aCC-BY 4.0 International license.

downstream ORF (ORF-2) encodes the structural polyprotein that is processed into the capsid protein, E3, E2, 6K, and E1.

While negative strand replication is initiated at the 3' end of the virus genome, as with many positive single stranded RNA viruses, regulatory elements and interactions within the 5' end of the CHIKV genome are required for its initiation and regulation [7]. We and others have previously demonstrated that such regulatory elements include functional RNA secondary structures and higher order interactions within the CHIKV 5'UTR and adjacent upstream region of ORF-1 (**Fig. 1B**). It has been speculated that these RNA elements may regulate template specificity and temporal control of switching, between CHIKV translation and genome replication [8, 9].

In a previously published study, we demonstrated by SHAPE mapping and reverse genetic analysis that the CHIKV 5'UTR and adjacent ORF-1 coding region is highly structured [9]. However, the study also highlighted a single-stranded region (nts 63-69) that exhibited very high SHAPE reactivity (associated with unpaired bases) and was located immediately between two RNA structures, that we demonstrated were essential for initiation of CHIKV genome replication **(Fig 1B)**. Interestingly, *in silico* analysis noted that nts ^{63}AUUAAU^{68} were closely homologous to the Musashi RNA binding protein (MSI) consensus binding sequence ((G/A)U_{1-3}AGU). MSI are highly conserved RNA binding proteins, containing two highly conserved tandem RNA recognition motifs (RNP-1 and RNP-2), that interact with RNA via the same consensus binding motif. Two MSI homologues have been identified, MSI-1 and MSI-2, that share over 90% homology in their RNA-binding domains and a high degree of

bioRxiv preprint doi: https://doi.org/10.1101/2023.03.29.534719; this version posted March 29, 2023. The copyright holder for this preprint (which was not certified by peer review) is the author/funder, who has granted bioRxiv a license to display the preprint in perpetuity. It is made available under aCC-BY 4.0 International license.

functional complementarity and redundancy [10, 11]. MSI have key roles in post-transcriptional regulation of genes involved in development, cell cycle regulation and maintenance of adult neural stem/progenitor cells [12]. A recent study demonstrated that MSI-1 promotes Zika Virus (ZIKV) genome replication in neurons, via interaction with the consensus binding site within the viral 3'UTR [13].

In the current study, we demonstrate through a range of infectious clone and sub-genomic replicon reporter assays that MSI-2 is required for efficient CHIKV genome replication. A small molecule inhibitor of MSI-1 and MSI-2 reduced infectious virus production by inhibition of CHIKV genome replication. Similarly, MSI-2 silencing by shRNA and siRNA inhibited both infectious virus production and genome replication, while co-silencing of both MSI-2 and MSI-1 resulted in a synergistic increase in inhibition of CHIKV replication. Reverse genetic analysis, in which the putative MSI binding site within the CHIKV 5'UTR was mutated, completely prevented rescue of mutant virus and inhibited CHIKV genome replication. Biochemical MSI-2 binding analysis by competition electromobility shift assay (EMSA) demonstrated that recombinantly expressed MSI-2 specifically interacts with the 5' region of the CHIKV genome and that this interaction is inhibited by mutation of the putative MSI 5'UTR binding site. These findings demonstrate for the first time that interaction between MSI and a binding site within the 5'UTR are required for replication of the CHIKV genome.

Materials and Methods

bioRxiv preprint doi: https://doi.org/10.1101/2023.03.29.534719; this version posted March 29, 2023. The copyright holder for this preprint (which was not certified by peer review) is the author/funder, who has granted bioRxiv a license to display the preprint in perpetuity. It is made available under aCC-BY 4.0 International license.

Cell culture

Human Rhabdomyosarcoma (RD), Human hepatoma (Huh7), Baby Hamster Kidney (BHK) and Human Embryonic Kidney (HEK) 293 were grown in Dulbecco's modified eagle's medium (DMEM; Sigma) containing 10% fetal bovine serum (FBS; PAA), 1x penicillin-streptomycin (Sigma), 25mM HEPES in 0.85% NaCl (Lonza) and 1% non-essential amino acids mixture (NEAA; Lonza). Cells were harvested using trypsin/EDTA, seeded at dilutions of 1:3 to 1:10 and maintained at 37°C in 5% CO_2.

CHIKV cDNA plasmid

The infectious CHIKV (ICRES), CHIKV Dual-luciferase sub-genomic replicon (CHIKV-SGR) and *trans*-complementation (pCHIKV-nsP1234 and pCHIK-Fluc/Gluc) assay were derived from the CHIKV ESCA strain, isolate LR2006 OPY1 (accession number DQ443544)[14]. In CHIKV-SGR the second ORF was replaced by a firefly luciferase gene and a *Renilla* luciferase gene was fused within nsP3 [15]. The *trans*-complementation assay utilised a CMV codon optimised plasmid to supply the CHIKV replicase in *trans* (pCHIKV-nsP1234) and a Pol II expressed reporter plasmid (pCHIKV-FLuc/GLuc), in which the majority of ORF-1 (downstream of nt 320) was replaced by a firefly luciferase gene and all of ORF-2 by a Gaussia Luciferase gene [16]. Plasmid cDNA was purified using GeneJET Plasmid Maxiprep kits (Thermo Fisher Scientific) according to the manufacturer's instructions.

Virus production

1×10^6 BHK cells were trypsinised and resuspended in 400 µl ice-cold DEPC-PBS. Cells were then electroporated with 1 µg 5′-capped CHIKV ICRES *in vitro* transcribed RNA

bioRxiv preprint doi: https://doi.org/10.1101/2023.03.29.534719; this version posted March 29, 2023. The copyright holder for this preprint (which was not certified by peer review) is the author/funder, who has granted bioRxiv a license to display the preprint in perpetuity. It is made available under aCC-BY 4.0 International license.

in a 4 mm electro-cuvette, with a single square wave pulse at 260 V for 25 ms using a Bio-Rad electroporator, before seeding into a T175 flask in 20 ml DMEM. After 24 h, supernatant was aspirated and virus titre measured by plaque assay on BHK cells.

CHIKV quantification by plaque assay

BHK cells were seeded at 1×10^5 cells per well in 12-well plates and maintained overnight in 1 ml DMEM. The following day monolayers were washed with PBS, infected with 10-fold serial dilutions of CHIKV transfection supernatant and maintained at 37 °C. 1 hpi monolayers were washed with PBS and covered with a 0.8% methylcellulose DMEM P/S overlay. 48 hpi monolayers were fixed and stained (5% paraformaldehyde and 0.25% crystal violet respectively), plaques counted and virus titres expressed in plaque-forming units per ml (PFU/ml).

Ro 08-2750 cell viability assay

RD cells were seeded in 96-well plate at $8x10^4$ cells/well and maintained for 24 hrs. Monolayers were then treated with increasing doses (0, 0.5, 1, 3, 5, 7, 10, 20 µM) of Ro 08-2750 (TOCRIS) dissolved in DMSO. After 24 hrs media/inhibitor was aspirated and replaced with 20 µl of 5 mg/mL 3-(4,5-dimethylthiazol-2-yl)-2,5-diphenyltetrazolium bromide (MTT) (Sigma) and incubated at 37 °C in 5% CO_2 for 3 hrs. After incubation, MTT solution was replaced with 100 µl DMSO and the plate shaken at 60 rpm for 5 min. Absorbance at 570 nm was determined using an Infinite F50 microplate reader (Tecan) and expressed as a percentage of DMSO control cells.

bioRxiv preprint doi: https://doi.org/10.1101/2023.03.29.534719; this version posted March 29, 2023. The copyright holder for this preprint (which was not certified by peer review) is the author/funder, who has granted bioRxiv a license to display the preprint in perpetuity. It is made available under aCC-BY 4.0 International license.

5 µM Ro 08-2750 was estimated to be the maximum non-toxic dose in in Huh7 cells and was used for all further assays.

Infectious CHIKV Ro 08-2750 inhibition assays

RD cells were seeded in 12-well plates at $1x10^5$ cells/well and incubated overnight in the presence of Ro 08-2750. Monolayers were then infected with CHIKV at MOI=0.1 and adsorbed to the cells for 1 h at 37°C before aspirating and maintaining in the presence of Ro 08-2750 for 24 hrs. Supernatants was then collected and infectious virus production measured by plaque assay.

siRNA depletion of MSI-1 and MSi-2

RD or Huh7 cells were seeded at $1x10^5$ cell/well in 12-well plates in antibiotic-free medium. After 24 hrs, cells were washed with PBS and incubated with 1x Opti-MEM + GlutaMAX (Gibco) for 20 min at 37°C/5% CO_2. For each well, 50 pmol MSI-1 (sc-106836; Santa Cruz) and/or MSI-2 siRNA (sc-75834; Santa Cruz) were mixed with 100 µl Opti-MEM and incubated at room temperature for 1min. No siRNAs were added to mock samples and 50 pmol of scrambled siRNA (SI03650318; QIAGEN) was used as a negative control. In parallel, 3 µl Lipofectamine RNAiMAX (Invitrogen) was mixed with 100 µl Opti-MEM and incubated at room temperature for 1 min. The siRNA and Lipofectamine RNAiMAX were mixed and incubated at room temperature for 5 min before adding to the cells. After 24 hrs, cells were either lysed to confirm MSI-1 or MSi-2 depletion by western blot or used for subsequent CHIKV infection assays.

bioRxiv preprint doi: https://doi.org/10.1101/2023.03.29.534719; this version posted March 29, 2023. The copyright holder for this preprint (which was not certified by peer review) is the author/funder, who has granted bioRxiv a license to display the preprint in perpetuity. It is made available under aCC-BY 4.0 International license.

shRNA depletion of MSI-1 and MSi-2

Human embryonic kidney 293 (HEK 293T) cells were plated in antibiotic-free DMEM in 6-well plates and maintained until confluency reached ~80%. For each transfection, in a single tube 300 µL OptiMEM was mixed with 1 µg p8.9 packaging plasmids, 1 µg envelope plasmid and either 1.5 µg MSI-2 shRNA or scrambled shRNA (Santa Cruz Biotechnology); in another tube, 300 µL of OptiMEM was mixed with 5 µL lipofectamine 2000 (Invitrogen). Both tubes were gently mixed by flicking, incubated at room temperature for 5 min, mixed together and incubated for 20 min at room temperature. The antibiotic-free DMEM was aspirated and the monolayers washed once with PBS. 800 µL Opti-MEM was added to each well before dropwise addition of the lentiviral plasmids/shRNA mixture. After maintenance at 37°C for 6 hrs the media was changed to antibiotic-free DMEM. 48 hpt the lentivirus containing supernatant was harvested and filtered through a 0.45 µm filter.

RD cells were seeded at $1x10^5$ cells/well the day prior to transduction. 1 mL of the lentivirus supernatant and polybrene (MERCK) were added to each well and incubated for 6 hrs before aspirating and replacing with antibiotic free DMEM. After 72 hrs media was replaced with DMEM containing 2.5 µg/ml puromycin, in which the cells were then maintained. The efficiency of the shRNA MSI-2 depletion was confirmed by western blot.

bioRxiv preprint doi: https://doi.org/10.1101/2023.03.29.534719; this version posted March 29, 2023. The copyright holder for this preprint (which was not certified by peer review) is the author/funder, who has granted bioRxiv a license to display the preprint in perpetuity. It is made available under aCC-BY 4.0 International license.

208 **Strand-specific Quantification of CHIKV RNA**

209 Total RNA was extracted from infected cells using TRI Reagent Solution (Applied
210 Biosystems) according to the manufacturer's instructions. Strand-specific RT-qPCR
211 (ssRT-qPCR) was performed as previously described [17]. Briefly, 500 ng of RNA was
212 reverse-transcribed with gene specific primers (Supplementary information 1) using
213 the SCRIPT cDNA Synthesis Kit (Jena Bioscience) according to the manufacturer's
214 protocol. 100 ng of strand-specific cDNA was used as template for the quantitative
215 PCR performed with the qPCRBIO SyGreen Blue Mix Lo-ROX (PCR Biosystems), with
216 gene specific primers amplifying a 94 bp region of the CHIKV nsP1-encoding
217 sequence using the following PCR program: 95°C for 2 mins, 40 x (95°C for 5 sec,
218 60°C for 30 sec), dissociation curve 60°C-95°C as pre-defined by the Mx3005P
219 thermal cycler (Agilent technologies). *In vitro* transcribed CHIKV ICRES RNA was
220 reverse transcribed and a cDNA dilution series employed as a standard to quantify
221 copy numbers in the respective samples.

222

223 ***In vitro* RNA transcription**

224 To generate CHIKV-SGR and infectious CHIKV RNA, 2 µg of cDNA was linearised with
225 Not-I HF and used as a template for transcription of 5' [m7G(5')ppp(5')G] capped
226 (m7G capped) RNA, using an SP6 mMessage mMachine kit, according to the
227 manufacturer's instructions (Life Technologies). Uncapped CHIKV 1–337 RNA, used
228 1 µg of CHIKV 1–337 PCR DNA as a template for *in vitro* transcription using the SP6-
229 Scribe™ standard RNA IVT kit, according to the manufacturer's instructions (Lucigen).

bioRxiv preprint doi: https://doi.org/10.1101/2023.03.29.534719; this version posted March 29, 2023. The copyright holder for this preprint (which was not certified by peer review) is the author/funder, who has granted bioRxiv a license to display the preprint in perpetuity. It is made available under aCC-BY 4.0 International license.

In all cases, following DNase I treatment, RNA was purified by LiCl precipitation and analysed by denaturing agarose gel electrophoresis.

CHIKV Sub-genomic replicon assays

For analysis of Ro 08-2750 inhibition, RD cells were seeded in 24 well plates at 5×10^4 cells per well and maintained overnight in the presence of Ro 08-2750. Monolayers were washed once in PBS before addition of 400 µl opti-Mem reduced-serum media and 100 µl transfection media. Transfection media was prepared according to the manufacturer's instructions, using 1 µl Lipofectamine 2000 (Invitrogen), 250 ng of CHIKV-SGR RNA and appropriate concentrations of Ro 08-2750, before being made up to 100 µl using opti-Mem. Monolayers were maintained for 6 hpt before the media was aspirated and replaced with complete DMEM/Ro 08-2750. At 8 and 24 hpt monolayers were lysed with 100 µl 1 x passive lysis buffer according to the manufacturer's instructions (Promega), stored at −80 °C and analysed using Dual-luciferase substrate (Promega) in a FLUOstar Optima luminometer (BMG labTech). For shRNA MSI-2 depleted cell lines the same method was followed, with the exclusion of Ro 08-2750.

***Trans*-complementation Assay**

The *trans*-complementation assay was performed as previously described [18]. Briefly, for analysis of Ro 08-2750 inhibition, RD cells were seeded in 12 well plates at 5×10^4 cells per well and maintained overnight in the presence of Ro 08-2750. Monolayers were then co-transfected with 1 µg each of the pCHIKV-nsP1234 and

bioRxiv preprint doi: https://doi.org/10.1101/2023.03.29.534719; this version posted March 29, 2023. The copyright holder for this preprint (which was not certified by peer review) is the author/funder, who has granted bioRxiv a license to display the preprint in perpetuity. It is made available under aCC-BY 4.0 International license.

pCHIKV-FLuc/GLuc using Lipofectamine 2000, as described previously, and assayed at 8 and 24 hpt. For shRNA MSI-2 depleted cell lines the same method was followed, with the exclusion of Ro 08-2750.

Expression and purification of recombinant MSI-2 RNA binding domains

The MSI-2 RNA binding domain expressing plasmid pET-22HT-MSI-2 (amino acid 8-193) was a kind gift from Prof S. Ryder (Addgene plasmid # 60356; http://n2t.net/addgene:60356; RRID: Addgene_60356) [19]. The plasmid was transformed into BL21 (DE3) competent cells following the manufacturer's protocol (NEB), a single colony was inoculated into 10 mL LB ampicillin (10 mg/ml) and incubated overnight at 37°C before inoculating 1000 ml 1 LB (ampicillin (10 mg/ml) and adding 100 µM Isopropyl β-D-1-thiogalactopyranoside (IPTG; Thermo Fisher Scientific) when the optical density reached 0.8. The culture was then incubated overnight at 18°C in an orbital shaker before centrifugation to pellet the bacteria. The pellet was resuspended in lysis buffer (20U/mL DNase I, 0.6U/mL RNase A, 1mg/mL lysozyme and 1x protease inhibitor) and lysed on ice for 30 min . Following sonication, the suspension was centrifuged twice at 2000 xg for 1 hour at 4°C. The was filtered through a 0.45 µm filter and His-MSI-2 was purified with HisTrap^{TM} FF column (Cytiva) using the Econo Gradient Pump (BIORAD) according to the manufacturer's protocol and overnight dialysis. The purified protein was quantified and the purity and identity assayed by Coomassie SDS-PAGE and western blot (Supplementary data 2).

bioRxiv preprint doi: https://doi.org/10.1101/2023.03.29.534719; this version posted March 29, 2023. The copyright holder for this preprint (which was not certified by peer review) is the author/funder, who has granted bioRxiv a license to display the preprint in perpetuity. It is made available under aCC-BY 4.0 International license.

After desalting using PD-10 desalting columns (Cytiva), His-MSI-2 protein was further purified by ion exchange chromatography. Following the manufacturer's instructions, the column was equilibrated with wash buffer (50 mM MES, 10 mM NaCl, pH 5.6, degassed) and the protein eluted in the same buffer. Ion exchange chromatography was performed using HiTrap SP HP cation exchange chromatography column (Cytiva) following the manufacturer's instructions and eluted in degassed 50mM MES, 1M NaCl, pH 5.6. The eluted protein fractions were analysed by Coomassie SDS-PAGE and western blot (Supplementary data 2).

^{32}P RNA end labelling

In vitro transcribed CHIKV RNA (nt's 1-337) was 5' dephosphorylated using Quick CIP according to the manufacturer's instructions (NEB) before purification using an RNA Clean & Concentrator column (Zymo Research). 20 pmoles of dephosphorylated RNA was combined with 2 µl 10 x T4 Polynucleotide Kinase buffer (NEB), 3 µl ATP(γ-^{32}P) 10 mCi/ml, 1 µl T4 Polynucleotide Kinase (NEB) and nuclease free H_2O to a final volume of 20 µl, incubated at 37 °C for 60 min, 65 °C for 20 min, purified using an RNA Clean & Concentrator Kit (Zymo Research) and resuspended in RNase-free H_2O.

Electromobility shift assay (EMSA)

RNA was incubated at 95°C for 2 min and on ice for 2 min before 3.3 x RNA folding buffer (100 mM HEPES pH 8.0, 100 mM NaCl and 10 mM MgCl2) and RNasin Plus RNase Inhibitor (Promega) was added to a final volume of 10 µl and incubated for 20 min at 37°C. MSI-2 protein was combined with 3.3 x RNA folding buffer, 0.5 x TE, 100% glycerol, RNasin Plus RNase Inhibitor (Promega) and 5 µg yeast tRNA as non-

bioRxiv preprint doi: https://doi.org/10.1101/2023.03.29.534719; this version posted March 29, 2023. The copyright holder for this preprint (which was not certified by peer review) is the author/funder, who has granted bioRxiv a license to display the preprint in perpetuity. It is made available under aCC-BY 4.0 International license.

specific competitor and incubated at 37°C for 2 min before adding to the RNA mixture and further incubation at 37°C for 15 min. Finally, samples were analysed by native PAGE gel electrophoresis at 135 V for ~2 h. The gel was fixed for 30 min and dried with gel dryer (BIORAD), exposed onto Hyperfilm™ ECL™ (Merck) and visualised using a Xograph Film Processor. Band shifts were quantified by densitometry, as a percentage of band density normalised to the total lane density, relative to control lanes.

Assessment of MSI-1, MSI-2 and CHIKV protein expression by western blot

Following infection and incubation, monolayers were lysed in IP lysis buffer (Promega) and incubated at room temperature for 30 min. Protein concentration was quantified using a Pierce™ BCA Protein Assay Kit (Thermo scientific) according to the manufacturer's instructions. Equal amounts of protein lysate were analysed by SDS-PAGE. Protein was transferred onto an Immobilon-FL PVFD transfer membrane (MERCK) using a TE77X semi-dry transfer (Hoefer) at 15 V for 60 min. Membranes were blocked using diluted Odyssey® Blocking Buffer in PBS (LI-COR) for 30 min and probed with primary antibodies against β-actin (1:10,000, mouse monoclonal, Sigma-Aldrich A1978), MSI-2 (1:1000 rabbit monoclonal, Abcam ab76148) and MSI-1 (1:5000, Abcam ab21628) in diluted Odyssey® Blocking Buffer in PBS (LI-COR) overnight at 4 °C. After overnight incubation, primary antibody was removed and membranes washed 3 times using PBS. Membranes were stained with secondary antibodies (IRDye® 800CW Donkey anti-Mouse; IRDye® 680LT Donkey anti-Rabbit; Li-

bioRxiv preprint doi: https://doi.org/10.1101/2023.03.29.534719; this version posted March 29, 2023. The copyright holder for this preprint (which was not certified by peer review) is the author/funder, who has granted bioRxiv a license to display the preprint in perpetuity. It is made available under aCC-BY 4.0 International license.

Cor) for 1 h at room temperature, washed 3 times using 1 x PBS, dried and then imaged using an Odyssey® Fc Imaging System (Li-Cor).

Statistical analysis

Statistical analysis was carried out using one-way ANOVA and Dunnett's multiple comparisons test on GraphPad Prism version 8.4.0. *P* values of ≤0.05 (*), ≤0.01 (**), ≤0.001 (***) were used to represent degrees of significance between each drug treatment/silencing/mutant to wild-type assay.

RESULTS

Ro inhibited replication of CHIKV infectious virus and sub-genomic replicon:

In order to investigate the potential role of MSI on CHIKV replication, we first assessed the effect of a well-characterised MSI small molecule inhibitor, Ro 08-2750 (Ro), on CHIKV productive replication in RD cells using both CHIKV infectious virus and a sub-genomic replicon (SGR) assay (Fig 2A). A number of studies have demonstrated that Ro interacts with the MSI RNA binding domains and acts as a competitive inhibitor for its RNA binding activity and subsequent MSI functions within the cell [20, 21] [22]. In the current study Ro was used at a maximum non-toxic dose as determined by MTT assay (Supplementary data 3).

The effect of Ro on productive CHIKV infection was measured at 8 and 24 hpi and it was observed that pre-treatment and incubation in the presence Ro significantly

bioRxiv preprint doi: https://doi.org/10.1101/2023.03.29.534719; this version posted March 29, 2023. The copyright holder for this preprint (which was not certified by peer review) is the author/funder, who has granted bioRxiv a license to display the preprint in perpetuity. It is made available under aCC-BY 4.0 International license.

345 inhibited infectious CHIKV replication by ~10-fold, relative to DMSO treated negative
346 controls (Fig. 2B). In order to investigate the effect of Ro on specific stages of CHIKV
347 replication we used an SGR construct, in which ORF-2 was replaced by a firefly
348 luciferase (FLuc) gene and a *Renilla* luciferase (Rluc) gene was fused in-frame with
349 ORF-1 nsP3 (Fig 2A)[9]. The SGR assay enabled us to measure the effect of Ro on
350 CHIKV genome replication and translation, in isolation of other stages of virus
351 infection, such as entry or egress. SGR ORF-1 and ORF-2 expression was significantly
352 inhibited at both 8 and 24 hpt, relative to DMSO treated negative controls, indicating
353 that Ro was inhibiting CHIKV replication at the level of virus genome replication or
354 translation (Fig 2C). ORF-1 is translated from full-length genomic transcripts and ORF-
355 2 from 18S sub-genomic transcripts. The observed inhibition of both ORF-1 and ORF-
356 2 expression was consistent with Ro acting at a stage of the replication cycle common
357 to expression of both ORFs.
358
359 **Ro inhibited CHIKV *trans*-complementation assay:**
360 Inhibition of SGR replication demonstrated that Ro was inhibiting CHIKV replication
361 at the level of virus genome replication or translation. In order to dissect this further,
362 we utilised a *trans*-complementation assay, that enabled the measurement of CHIKV
363 genome replication in isolation of virus translation (Fig 3A)[23]. The *trans*-
364 complementation system utilised a codon-optimised CHIKV replicase-expressing
365 plasmid (pCHIKV-nsP1234), which expresses the virus nsPs from a CMV promoter.
366 The expressed nsPs replicate a CHIKV reporter construct (pCHIKV-FLuc/GLuc), in
367 which the majority of ORF-1 is replaced by an FLuc gene and ORF-2 by the Gaussia
368 luciferase (GLuc) gene. The effect of Ro on pCHIKV-FLuc/GLuc expression was

bioRxiv preprint doi: https://doi.org/10.1101/2023.03.29.534719; this version posted March 29, 2023. The copyright holder for this preprint (which was not certified by peer review) is the author/funder, who has granted bioRxiv a license to display the preprint in perpetuity. It is made available under aCC-BY 4.0 International license.

369 measured at 8 and 24 hpt in cells pre-treated with and maintained in the presence of
370 Ro. Both ORF-1 and ORF-2 expression was observed to be significantly inhibited
371 relative to the DMSO treated negative controls, indicating that Ro was inhibiting
372 CHIKV replication specifically at the level of virus genome replication.
373
374 **MSI-2 shRNA silencing inhibits infectious CHIKV replication:**
375 In order to confirm that Ro induced inhibition of CHIKV genome replication was due
376 to specific inhibition of MSI, rather than an unrecognised off target effect of Ro, we
377 next investigated CHIKV replication following shRNA silencing of MSI expression.
378 Analysis of RD cell total protein extract by western blot, demonstrated that MSI-2
379 was strongly expressed in RD cells while MSI-1 was expressed at a very low level
380 (Supplementary data 4). Consequently, we initially investigated the effect of specific
381 MSI-2 shRNA silencing on CHIKV replication. RD cells were transduced with lentiviral
382 vectors encoding shRNA against human MSI-2 and successful silencing was
383 confirmed by western blot (Fig 4A). Negative control cells were treated with either
384 transfection reagent only (mock) or non-specific scrambled shRNA. Following
385 infection of MSI-2 depleted and negative control cells, productive CHIKV infection
386 was measured by plaque assay at 8 and 24 hpi (Fig 4B). Strand specific qRT-PCR was
387 also used to measure levels of genomic (positive strand) and replication
388 intermediate (negative strand) CHIKV RNA at both time points (Fig 4 C and D). As
389 observed previously following treatment with Ro, relative to the scrambled shRNA
390 control productive CHIKV replication was significantly inhibited following shRNA MSI-
391 2 silencing (Fig 4B). Similarly, strand specific qRT-PCR demonstrated that both
392 genomic and replication intermediate CHIKV RNA levels were significantly inhibited

bioRxiv preprint doi: https://doi.org/10.1101/2023.03.29.534719; this version posted March 29, 2023. The copyright holder for this preprint (which was not certified by peer review) is the author/funder, who has granted bioRxiv a license to display the preprint in perpetuity. It is made available under aCC-BY 4.0 International license.

(Fig 4 C and D). These results are consistent with CHIKV requiring MSI-2 for efficient genome replication.

MSI-2 is required for efficient CHIKV genome replication

In order to confirm that MSI-2 silencing had the same effect on CHIKV genome replication as Ro small molecule inhibition, we repeated analysis with the SGR and *trans*-complementation systems, following shRNA silencing of MSI-2. As previously described, MSI-2 shRNA silenced RD cells were transfected with the SGR system and ORF-1 and ORF-2 expression measured by RLuc and FLuc expression at 8 and 24 hpt (Fig 5A and B). Expression of both ORF-1 and ORF-2 was significantly inhibited at both 8 and 24 hpt, consistent with an MSI-2 requirement for CHIKV genome replication or translation. Analysis at the same time points using the *trans*-complementation system, following shRNA MSI-2 silencing and measuring ORF1 and ORF2 expression, confirmed significant inhibition of CHIKV genome replication when measured in isolation of the effects of other stages of the virus replication cycle (Fig 5C and D)

Both MSI-2 and MSI-1 have a proviral effect on CHIKV genome replication:

While results clearly demonstrated that MSI-2 was required for efficient CHIKV replication, it remained unclear if MSI homologue MSI-1 was also agonistic for CHIKV replication. As previously described, western blot analysis showed that MSI-1 was not highly expressed in RD cells. Consequently, we analysed MSI homologue redundancy in Huh7 human hepatoma cells, in which both MSI-1 and MSI-2 homologues are strongly expressed (Supplementary data 4) and are highly

bioRxiv preprint doi: https://doi.org/10.1101/2023.03.29.534719; this version posted March 29, 2023. The copyright holder for this preprint (which was not certified by peer review) is the author/funder, who has granted bioRxiv a license to display the preprint in perpetuity. It is made available under aCC-BY 4.0 International license.

permissive for CHIKV replication [24]. Following individual and combined siRNA silencing of MSI-1 and MSI-2 in Huh7 cells (Supplementary data 5), CHIKV replication was assayed by plaque assay and ssRT-qPCR at 8 and 24 hpi (Fig 6A, B and C). As was observed for RD cells, MSI-2 silencing significantly inhibited CHIKV replication, measured by both plaque assay and strand specific ssRT-qPCR. Interestingly, it was observed that MSI-1 silencing in Huh7 cells had a similar significant inhibitory effect and that siRNA co-silencing of both MSI-1 and MSI-2 had a synergistic effect on inhibition of CHIKV replication. In concordance with previous results, siRNA silencing of MSI-2 in RD cells significantly inhibited CHIKV replication, by comparable levels observed following shRNA silencing and inhibition by Ro. Consistent with low MSI-1 expression in RD cells, siRNA co-silencing of both MSI-1 and MSI-2 did not significantly increase levels of CHIKV inhibition (Fig. 6D, E and F).

MSI-2 binds specifically to the predicted $_{63}$AUUAAU$_{68}$ 5'UTR MSI binding site in the CHIKV 5'UTR

Following confirmation that MSI-2 RNA binding protein is required for efficient CHIKV genome replication, we next used native EMSA to biochemically investigate the potential for a direct interaction between the RNA binding domains of MSI-2 and nucleotides $_{63}$AUUAAU$_{68}$ within the virus 5'UTR, which had close sequence homology to the (G/A)U$_{1-3}$AGU MSI consensus nucleotide binding motif [25]. $_{63}$AUUAAU$_{68}$ is located in single-stranded region of the 5' UTR, 9 nts upstream of the AUG start codon and between two RNA structures that are essential for CHIKV genome replication (Fig. 1B)[9]. The first 330nts of the CHIKV genome (RNA-330), representing the 5'UTR and adjacent upstream region of ORF1, was *in vitro*

bioRxiv preprint doi: https://doi.org/10.1101/2023.03.29.534719; this version posted March 29, 2023. The copyright holder for this preprint (which was not certified by peer review) is the author/funder, who has granted bioRxiv a license to display the preprint in perpetuity. It is made available under aCC-BY 4.0 International license.

transcribed, 5' end radiolabelled with ATP-[γ-32P] and incubated at 37°C - conditions under which correct folding of the functional RNA-330 structure was previously validated [9]. Following incubation with increasing concentrations of recombinantly expressed and purified MSI-2 8-193 in the presence of unlabelled tRNA, reaction products were separated by native PAGE and analysed by autoradiography (Fig 7A). Relative to unbound RNA-330, the presence of MSI-2 8-193 resulted in the retardation of RNA-330 migration during native PAGE, consistent with the formation of an RNA-330/MSI-2 8-193 complex. In order to investigate the specificity of the observed interaction, a fixed molar ratio of RNA-330$^{\gamma\text{-}32P}$ and MSI-2 8-193 was incubated with increasing concentrations of competitor unlabelled RNA-330 (Fig 7B). Increasing concentrations of unlabelled RNA-330 reduced the formation of the RNA-330$^{\gamma\text{-}32P}$/MSI-2 8-193 complex, with a corresponding increase in unbound RNA-330$^{\gamma\text{-}32P}$.

In order to further confirm the specificity and location of the interaction the putative MSI-2 binding site $_{63}$AUUAAU$_{68}$ was mutated to $_{63}$CAACUU$_{68}$ (henceforth termed $_{63}$CAACUU$_{68}$-mut). EMSA competition with unlabelled $_{63}$CAACUU$_{68}$-mut RNA-330 was significantly less efficient at competing for MSI-2 8-193 binding than wild-type CHIKV RNA (Fig 7 C and D). These ESMA results are consistent with an interaction between MSI-2 and the upstream region of the CHIKV genome. The significant inhibition of this interaction in the $_{63}$CAACUU$_{68}$-mut indicated both that the interaction was specific and that nts $_{63}$AUUAAU$_{68}$ function as an MSI binding motif.

bioRxiv preprint doi: https://doi.org/10.1101/2023.03.29.534719; this version posted March 29, 2023. The copyright holder for this preprint (which was not certified by peer review) is the author/funder, who has granted bioRxiv a license to display the preprint in perpetuity. It is made available under aCC-BY 4.0 International license.

Mutagenesis of 5'UTR $_{63}$AUUAAU$_{68}$ MSI binding site inhibits CHIKV genome replication and prevents virus rescue

In order to further investigate the role of the $_{63}$AUUAAU$_{68}$ MSI binding motif in CHIKV replication, we took a reverse genetic approach, in which the $_{63}$AUUAAU$_{68}$>$_{63}$CAACUU$_{68}$ mutations were incorporated into both the *trans*-complementation assay and infectious CHIKV. Similar to previous results following MSI inhibition, expression of both ORF-1 and ORF-2 from the *trans*-complementation system were significantly inhibited in $_{63}$CAACUU$_{68}$-mut relative to the wild type at 8 and 24 hpt (Fig 8A and B); indicating that mutation of the putative MSI binding site significantly inhibited CHIKV at the level of virus genome replication. Interestingly, despite repeated attempts, we were not able to rescue infectious CHIKV $_{63}$CAACUU$_{68}$-mut virus, indicating that disruption of the potential MSI binding site completely inhibited infectious CHIKV replication (Fig 8C).

DISCUSSION

For the first time, in this study we demonstrate that cellular RNA binding protein MSI is required for efficient CHIKV replication. Our data demonstrates that MSI-2 interacts directly with the 5' end of the CHIKV genome and is consistent with an interaction at position $_{63}$AUUAAU$_{68}$. A single-stranded region located between two conserved stem-loops and immediately upstream of the AUG start codon (Fig 1) [9]. Inhibition of MSI-2 expression by siRNA or shRNA, its RNA-binding activity by Ro and reverse genetic disruption of the CHIKV-5'UTR/MSI-2 interaction, inhibited CHIKV

bioRxiv preprint doi: https://doi.org/10.1101/2023.03.29.534719; this version posted March 29, 2023. The copyright holder for this preprint (which was not certified by peer review) is the author/funder, who has granted bioRxiv a license to display the preprint in perpetuity. It is made available under aCC-BY 4.0 International license.

replication at the level of virus genome replication. In further analysis, we demonstrated that depletion of both MSI-1 and MSI-2 homologues resulted in a synergistic increase in the level of CHIKV inhibition, supporting the premise that both MSI homologues have a redundant pro-viral effect on CHIKV replication.

While depletion of MSI-2 by siRNA and shRNA clearly demonstrated significant inhibition of CHIKV replication, measured by infectious virus production, CHIKV-SGR replication or a *trans*-complementation assay, we did not observe complete inhibition of virus replication. Western blot analysis indicated that we did not achieve complete ablation of MSI-2 expression by either siRNA or shRNA, presumably reducing the level of CHIKV inhibition observed. We demonstrated by western blot that in RD cells MSI-2 is expressed to a high level but the MSI-1 homologue is only expressed to a low level. However, given the synergistic effect that we observed when silencing expression of both MSI-2 and MSI-1 in Huh7 cells (in which both are expressed to high levels), the ability of MSI homologues to complement for each other may also have reduced the level of CHIKV inhibition observed. This hypothesis is consistent with reverse genetic results, in which mutation of the $_{63}$AUUAAU$_{68}$ MSI binding site, dramatically inhibited the CHIKV-5'UTR/MSI-2 binding affinity and completely prevented rescue of mutant virus.

Translation and replication of positive-sense RNA virus genomes, such as those of CHIKV are mutually exclusive processes – with translation initiating at the 5' end of the genome and replication at the 3'. Consequently, it is essential that such viruses have mechanisms for temporal control of both processes. In many such viruses (e.g.

bioRxiv preprint doi: https://doi.org/10.1101/2023.03.29.534719; this version posted March 29, 2023. The copyright holder for this preprint (which was not certified by peer review) is the author/funder, who has granted bioRxiv a license to display the preprint in perpetuity. It is made available under aCC-BY 4.0 International license.

Hepatitis C virus and Polio virus) control involves dynamic interactions between RNA structures in the virus genome and host/virally expressed protein complexes [7]. The mechanisms and interactions which CHIKV and other alphaviruses use for temporal control of genome translation and replication remain unclear. However, a recent study suggested a crucial role for the cellular helicase DHX9. Matkovic et al, demonstrated that interaction between DHX9 and the 5' end of the virus genome upregulates CHIKV ORF-1 non-structural protein translation, while simultaneously inhibiting replication of its genome [26]. Build-up of nsP2 caused proteosome induced degradation of DHX9, although the detailed mechanism for this remains unclear.

While, genome replication of positive-sense RNA viruses initiates at the 3' end, it is commonly controlled by promoter elements and interactions with RNA binding proteins at the 5' end. Results described in this and previous studies are consistent with a model in which temporal control of CHIKV ORF-1 translation and genome replication is controlled by a mechanism involving interactions between DHX9, MSI2 and the 5' region of the virus genome. However, the dynamics and mechanism by which the opposing roles if MSI-2 and DHX-9 influence CHIKV replication and their interactions with the virus genome remains unclear and is the focus of ongoing studies.

In summary, using MSI-2 depletion and Ro small molecule inhibitor we demonstrate that MSI-2 RNA binding protein is a critical host factor for efficient CHIKV replication. Inhibition of ORF-1 and ORF-2 signal from the *trans*-complementation assay indicate

bioRxiv preprint doi: https://doi.org/10.1101/2023.03.29.534719; this version posted March 29, 2023. The copyright holder for this preprint (which was not certified by peer review) is the author/funder, who has granted bioRxiv a license to display the preprint in perpetuity. It is made available under aCC-BY 4.0 International license.

that MSI-2 is required at the level of CHIKV genome replication. Furthermore, EMSA and reverse genetic results are consistent with a direct interaction between MSI-2 and $_{63}$AUUAAU$_{68}$ in the positive genomic strand of the virus 5'UTR, suggesting a role in negative strand synthesis. Results from this study are important both for our understanding of the fundamental interactions essential to replication of this important human pathogen and for future studies towards specific antiviral therapies.

Funding

This work was supported by funding from the MRC to AT (MR/NO1054X/1).

Data availability statement

The data underlying this article will be shared on reasonable request to the corresponding author.

REFERENCES

1. Fong, S.W., R.M. Kini, and L.F.P. Ng, *Mosquito Saliva Reshapes Alphavirus Infection and Immunopathogenesis.* Journal of Virology, 2018. **92**(12).
2. McPherson, R.L., et al., *ADP-ribosylhydrolase activity of Chikungunya virus macrodomain is critical for virus replication and virulence.* Proceedings of the National Academy of Sciences of the United States of America, 2017. **114**(7): p. 1666-1671.
3. Petitdemange, C., N. Wauquier, and V. Vieillard, *Control of immunopathology during chikungunya virus infection.* Journal of Allergy and Clinical

bioRxiv preprint doi: https://doi.org/10.1101/2023.03.29.534719; this version posted March 29, 2023. The copyright holder for this preprint (which was not certified by peer review) is the author/funder, who has granted bioRxiv a license to display the preprint in perpetuity. It is made available under aCC-BY 4.0 International license.

Immunology, 2015. **135**(4): p. 846-855.

4. Ng, L.F., *Immunopathology of Chikungunya virus infection: lessons learned from patients and animal models.* Annual review of virology, 2017. **4**: p. 413-427.

5. Meshram, C.D., et al., *Multiple Host Factors Interact with the Hypervariable Domain of Chikungunya Virus nsP3 and Determine Viral Replication in Cell-Specific Mode.* J Virol, 2018. **92**(16).

6. Rupp, J.C., et al., *Alphavirus RNA synthesis and non-structural protein functions.* Journal of General Virology, 2015. **96**(9): p. 2483-2500.

7. Tuplin, A., *Diverse roles and interactions of RNA structures during the replication of positive-stranded RNA viruses of humans and animals.* J Gen Virol, 2015.

8. Frolov, I., R. HARDY, and C.M. RICE, *Cis-acting RNA elements at the 5′ end of Sindbis virus genome RNA regulate minus-and plus-strand RNA synthesis.* Rna, 2001. **7**(11): p. 1638-1651.

9. Kendall, C., et al., *Structural and phenotypic analysis of Chikungunya virus RNA replication elements.* Nucleic Acids Res, 2019. **47**(17): p. 9296-9312.

10. Troschel, F.M., et al., *Knockdown of Musashi RNA Binding Proteins Decreases Radioresistance but Enhances Cell Motility and Invasion in Triple-Negative Breast Cancer.* Int J Mol Sci, 2020. **21**(6).

11. Sutherland, J.M., et al., *RNA binding proteins in spermatogenesis: an in depth focus on the Musashi family.* Asian J Androl, 2015. **17**(4): p. 529-36.

12. Horisawa, K., et al., *The Musashi family RNA-binding proteins in stem cells.* Biomol Concepts, 2010. **1**(1): p. 59-66.

13. Chavali, P.L., et al., *Neurodevelopmental protein Musashi-1 interacts with the Zika genome and promotes viral replication.* Science, 2017. **357**(6346): p. 83-88.

14. Tsetsarkin, K., et al., *Infectious clones of Chikungunya virus (La Reunion isolate) for vector competence studies.* Vector Borne Zoonotic Dis, 2006. **6**(4): p. 325-37.

15. Pohjala, L., et al., *Inhibitors of alphavirus entry and replication identified with a stable Chikungunya replicon cell line and virus-based assays.* PloS one, 2011. **6**(12): p. e28923.

bioRxiv preprint doi: https://doi.org/10.1101/2023.03.29.534719; this version posted March 29, 2023. The copyright holder for this preprint (which was not certified by peer review) is the author/funder, who has granted bioRxiv a license to display the preprint in perpetuity. It is made available under aCC-BY 4.0 International license.

16. Lello, L.S., et al., *Cross-utilisation of template RNAs by alphavirus replicases.* PLoS Pathog, 2020. **16**(9): p. e1008825.
17. Muller, M., et al., *Chikungunya virus requires cellular chloride channels for efficient genome replication.* PLoS Negl Trop Dis, 2019. **13**(9): p. e0007703.
18. Bartholomeeusen, K., et al., *A Chikungunya Virus trans-Replicase System Reveals the Importance of Delayed Nonstructural Polyprotein Processing for Efficient Replication Complex Formation in Mosquito Cells.* J Virol, 2018. **92**(14).
19. Clingman, C.C., et al., *Allosteric inhibition of a stem cell RNA-binding protein by an intermediary metabolite.* Elife, 2014. **3**: p. e02848.
20. Arkin, M.R. and J.A. Wells, *Small-molecule inhibitors of protein–protein interactions: progressing towards the dream.* Nature reviews Drug discovery, 2004. **3**(4): p. 301-317.
21. Niederhauser, O., et al., *NGF ligand alters NGF signaling via p75NTR and TrkA.* Journal of neuroscience research, 2000. **61**(3): p. 263-272.
22. Minuesa, G., et al., *Small-molecule targeting of MUSASHI RNA-binding activity in acute myeloid leukemia.* Nature communications, 2019. **10**(1): p. 1-15.
23. Lello, L.S., et al., *Cross-utilisation of template RNAs by alphavirus replicases.* PLoS pathogens, 2020. **16**(9): p. e1008825.
24. Roberts, G.C., et al., *Evaluation of a range of mammalian and mosquito cell lines for use in Chikungunya virus research.* Scientific reports, 2017. **7**(1): p. 1-13.
25. Zearfoss, N.R., et al., *A conserved three-nucleotide core motif defines Musashi RNA binding specificity.* J Biol Chem, 2014. **289**(51): p. 35530-41.
26. Matkovic, R., et al., *The Host DHX9 DExH-Box Helicase Is Recruited to Chikungunya Virus Replication Complexes for Optimal Genomic RNA Translation.* Journal of Virology, 2019. **93**(4).

Figure Legends:

Figure 1. A) Schematic representation of CHIKV genome organisation **B)** Schematic representation of CHIKV RNA structures within the 5'UTR and adjacent ORF-1 region

bioRxiv preprint doi: https://doi.org/10.1101/2023.03.29.534719; this version posted March 29, 2023. The copyright holder for this preprint (which was not certified by peer review) is the author/funder, who has granted bioRxiv a license to display the preprint in perpetuity. It is made available under aCC-BY 4.0 International license.

of the CHIKV genome (Kendall et al., 2019). RNA replication elements SL3, SL47, SL88, SL102, SL165, SL194 and SL246 are labelled in black type. The ORF-1 AUG start codon is labelled by a green arrow and the putative MSI binding site by a red oval.

Figure 2. Ro signifyingly inhibits replication of infectious CHIKV and the CHIKV-SGR **A)** Schematic representations of CHIKV infectious clone (top) compared to the sub-genomic replicon (SGR) (bottom) in which a *Renilla* luciferase (RLuc) reporter gene is fused within the nsp3 coding sequence and the structural genes of ORF-2 are replaced by a firefly luciferase (Fluc) reporter gene. Replication is expressed in Relative Light Units [RLU] **B)** Ro significantly inhibits productive CHIKV productive replication relative to DMSO treated negative controls at 8 and 24 hpi. **C** and **D)** Ro 08-2750 significantly inhibits CHIKV-SGR replication, measured by both ORF-1 and ORF-2 expression, relative to DMSO treated negative controls at 8 and 24 hpt. N=3, error bars represent standard error from the mean and significance was measured by two-tailed T-test (* = $P < 0.05$, ** = $P < 0.01$, *** = $P < 0.001$).

Figure 3. Ro signifyingly inhibits CHIKV genome replication. **A)** Schematic representation of CHIKV *trans*-complementation assay showing codon optimised pCHIKV-nsP1234 (top) from which the CHIKV nsPs were translated and pCHIK-Fluc/Gluc (bottom) in which ORF-1 was replaced by an Fluc reporter gene, fused to the first 77 nts or CHIKV ORF-1 (N77) down-stream of the authentic CHIKV 5'UTR. ORF-2, flanked by the authentic intragenic (SG) and 3' UTRs, was replaced by a Gluc reporter gene. **B** and **C)** Ro significantly inhibited CHIKV genome replication of the *trans*-complementation assay, measured by both ORF-1 and ORF-2 expression, relative to DMSO treated negative controls at 8 and 24 hpt. N=3, error bars represent standard error from the mean and significance was measured by two-tailed T-test (* = $P < 0.05$, ** = $P < 0.01$, *** = $P < 0.001$).

Figure 4. shRNA suppression of MSI-2 significantly inhibits replication of infectious CHIKV. **A)** Western blot analysis of total cellular protein extracted from Rd cells and compared to negative control scrambled shRNA, demonstrated consistent shRNA

bioRxiv preprint doi: https://doi.org/10.1101/2023.03.29.534719; this version posted March 29, 2023. The copyright holder for this preprint (which was not certified by peer review) is the author/funder, who has granted bioRxiv a license to display the preprint in perpetuity. It is made available under aCC-BY 4.0 International license.

knockdown of MSI-2 over 3 serial passages (P1- P3). MSI-2 suppression significantly inhibited productive CHIKV replication, relative to scrambled shRNA at 8 and 24 hpi measured by plaque assay **B)** and strand specific qRT-PCR for the the virus genomic **C)** and negative intermediate **D)** strands. N=3, error bars represent standard error from the mean and significance was measured by two-tailed T-test (* = P < 0.05, ** = P < 0.01, *** = P < 0.001).

Figure 5. shRNA suppression of MSI-2 significantly inhibits CHIKV-SGR replication and CHIKV genome replication. **A** and **B)** shRNA suppression of MSI-2 significantly inhibited CHIKV-SGR replication, measured by both ORF-1 and ORF-2 expression, relative to scrambled shRNA negative controls at 8 and 24 hpt. **C** and **D)** shRNA suppression of MSI-2 significantly inhibited CHIKV genome replication of the *trans*-complementation assay, measured by both ORF-1 and ORF-2 expression, relative to DMSO treated negative controls at 8 and 24 hpt. N=3, error bars represent standard error from the mean and significance was measured by two-tailed T-test (* = P < 0.05, ** = P < 0.01, *** = P < 0.001).

Figure 6. siRNA Depletion of either MSI-1 or MSI-2 significantly inhibited CHIKV replication in Huh7 cells and co-depletion of both MSI-1 and MSI-2 had a synergistic effect on CHIKV inhibition in Huh7 cells. siRNA depletion of MSI-2 significantly inhibited CHIKV replication in RD cells and co-depletion of both MSI-1 and MSI-2 did not increase the level of CHIKV inhibition. siRNA depletion of MSI-1 and MSI-2 significantly inhibited CHIKV replication in Huh7 cells relative to scrambled siRNA at 8 and 24 hpi measured by plaque assay **A)** and strand specific qRT-PCR for the the virus genomic **B)** and negative intermediate **C)** strands. siRNA depletion of MSI-2 in RD cells significantly inhibited CHIKV replication in relative to scrambled siRNA at 8 and 24 hpi measured by plaque assay **D)** and strand specific qRT-PCR for the the virus genomic **E)** and negative intermediate **F)** strands. N=3, error bars represent standard error from the mean and significance was measured by two-tailed T-test (* = P < 0.05, ** = P < 0.01, *** = P < 0.001).

bioRxiv preprint doi: https://doi.org/10.1101/2023.03.29.534719; this version posted March 29, 2023. The copyright holder for this preprint (which was not certified by peer review) is the author/funder, who has granted bioRxiv a license to display the preprint in perpetuity. It is made available under aCC-BY 4.0 International license.

688 **Figure 7.** Native EMSAs between *in vitro* transcribed ^{32}P 5' radiolabeled CHIKV RNA
689 nts 1-330 (*RNA^{WT}) and recombinantly expressed MSI-2 demonstrated an
690 RNA/protein interaction that was outcompeted by increasing concentrations of
691 equivalent unlabeled (RNA^{WT}) but less efficiently by the same RNA incorporating
692 BSM mutation $_{63}$AUUAAU$_{68}$ >$_{63}$CAACUU$_{68}$ (RNA^{BSM}). **A)** Increasing concentrations of
693 MSI-2 intensified the observed band shift to the larger RNA/Protein complex and
694 decreased the equivalent unbound RNA band. The interaction between a 1:4 ratio of
695 *RNA^{WT}:MSI-2 was competed with increasing concentrations of unlabelled **B)** RNA^{WT}
696 or **C)** RNA^{mut} ($_{63}$CAACUU$_{68}$-mut). **D)** Band shifts in the unlabeled RNA competition
697 EMSAs were quantified by densitometry and expressed as % change in the density of
698 the RNA/Protein complex bands, normalized to the equivalent total lane density, for
699 each competition ratio and compared each time to ratio 1:0. N=3, error bars
700 represent standard error from the mean and significance was measured by two-
701 tailed T-test (* = P < 0.05, ** = P < 0.01, *** = P < 0.001). Grey block triangles
702 indicate increasing concentrations of specific reactants.
703
704 **Figure 8.** Substitutions within the predicted MSI binding site ($_{63}$CAACUU$_{68}$-mut)
705 prevented rescue of BSM-mutant virus and significantly inhibited CHIKV genome
706 replication. **A** and **B)** Mutation of the MSI binding site significantly inhibited CHIKV
707 genome replication of the *trans*-complementation assay, measured by both ORF-1
708 and ORF-2 expression, relative to wild-type positive controls at 8 and 24 hpt. **C)**
709 Mutation of the predicted MSI binding site prevented rescue of BSM-mutant CHIKV
710 following transfection of capped *in vitro* transcribed RNA into BHK cells. Released
711 virus was measured by plaque assay of supernatant 24 hpt and compared to positive
712 control wild-type infectious CHIKV *in vitro* transcribed RNA, which was transfected
713 and analysed in parallel. N=3, error bars represent standard error from the mean and
714 significance was measured by two-tailed T-test (* = P < 0.05, ** = P < 0.01, *** = P <
715 0.001).

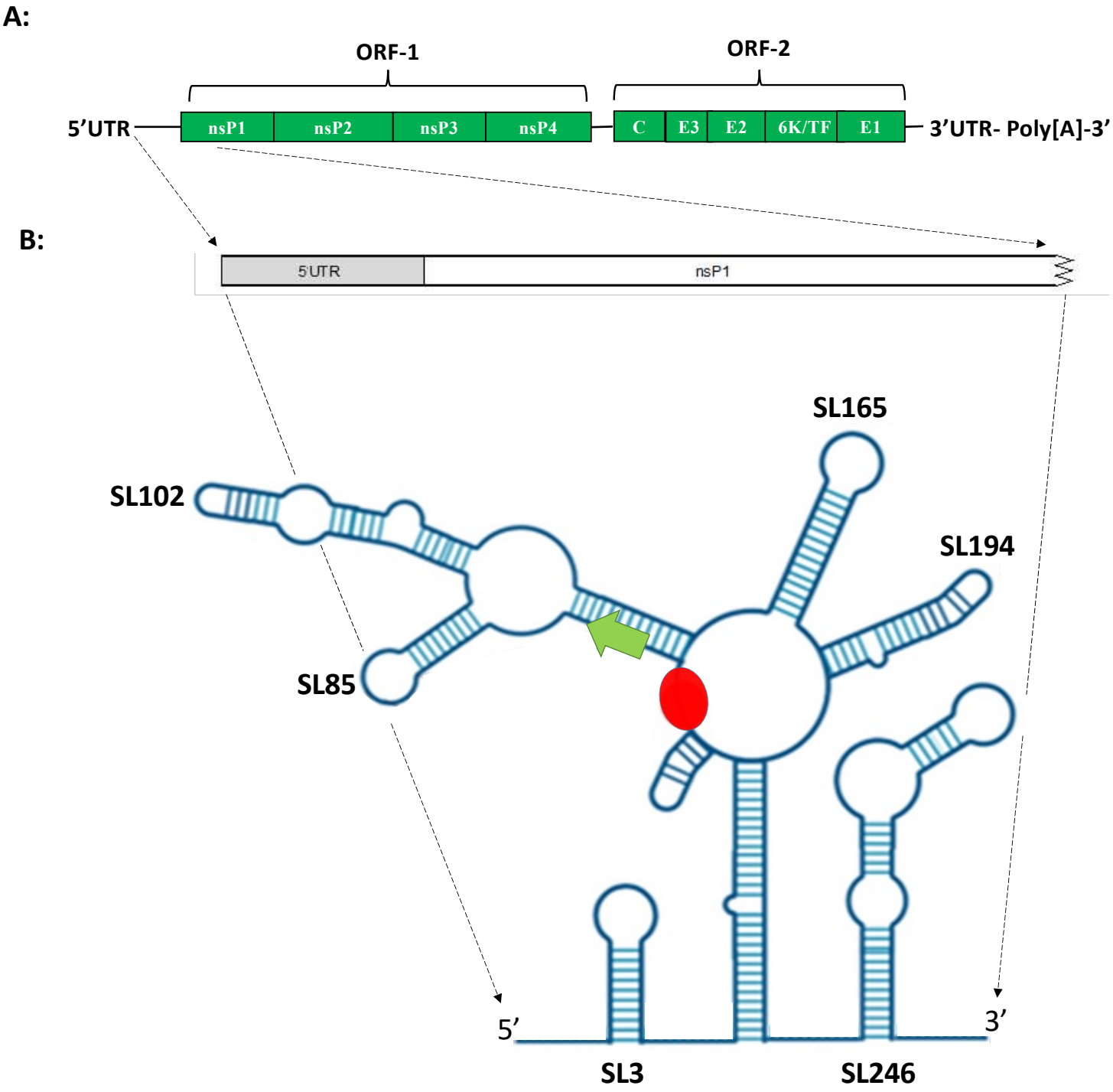

Figure 1. A) Schematic representation of CHIKV genome organisation **B)** Schematic representation of CHIKV RNA structures within the 5'UTR and adjacent ORF-1 region of the CHIKV genome (Kendall et al., 2019). RNA replication elements SL3, SL47, SL88, SL102, SL165, SL194 and SL246 are labelled in black type. The ORF-1 AUG start codon is labelled by a green arrow and the putative MSI binding site by a red oval

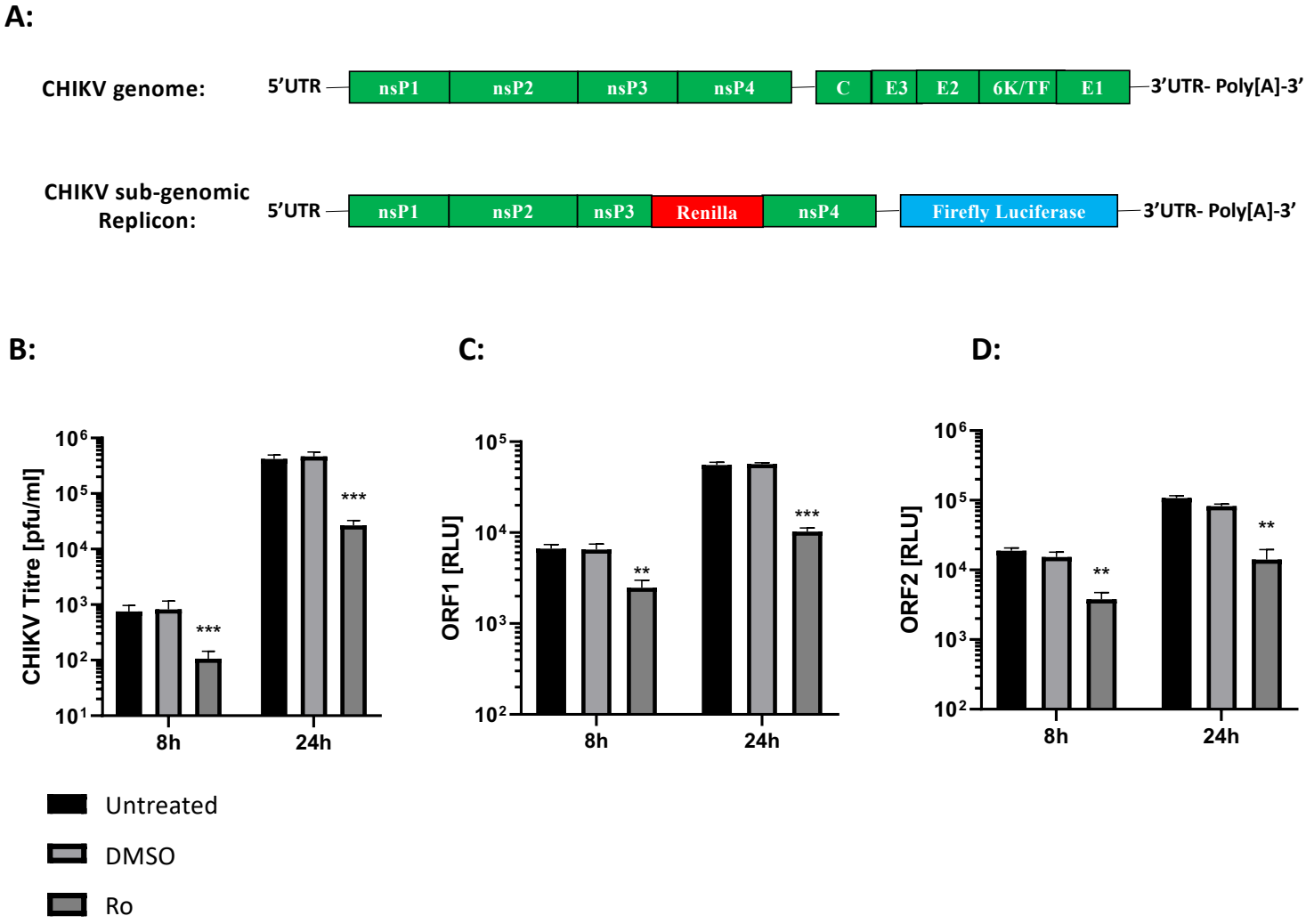

Figure 2. Ro signifyingly inhibits replication of infectious CHIKV and the CHIKV-SGR A) Schematic representations of CHIKV infectious clone (top) compared to the sub-genomic replicon (SGR) (bottom) in which a *Renilla* luciferase (RLuc) reporter gene is fused within the nsp3 coding sequence and the structural genes of ORF-2 are replaced by a firefly luciferase (Fluc) reporter gene. Replication is expressed in Relative Light Units [RLU] **B)** Ro significantly inhibits productive CHIKV productive replication relative to DMSO treated negative controls at 8 and 24 hpi. **C and D)** Ro 08-2750 significantly inhibits CHIKV-SGR replication, measured by both ORF-1 and ORF-2 expression, relative to DMSO treated negative controls at 8 and 24 hpt. N=3, error bars represent standard error from the mean and significance was measured by two-tailed T-test (* = $P < 0.05$, ** = $P < 0.01$, *** = $P < 0.001$).

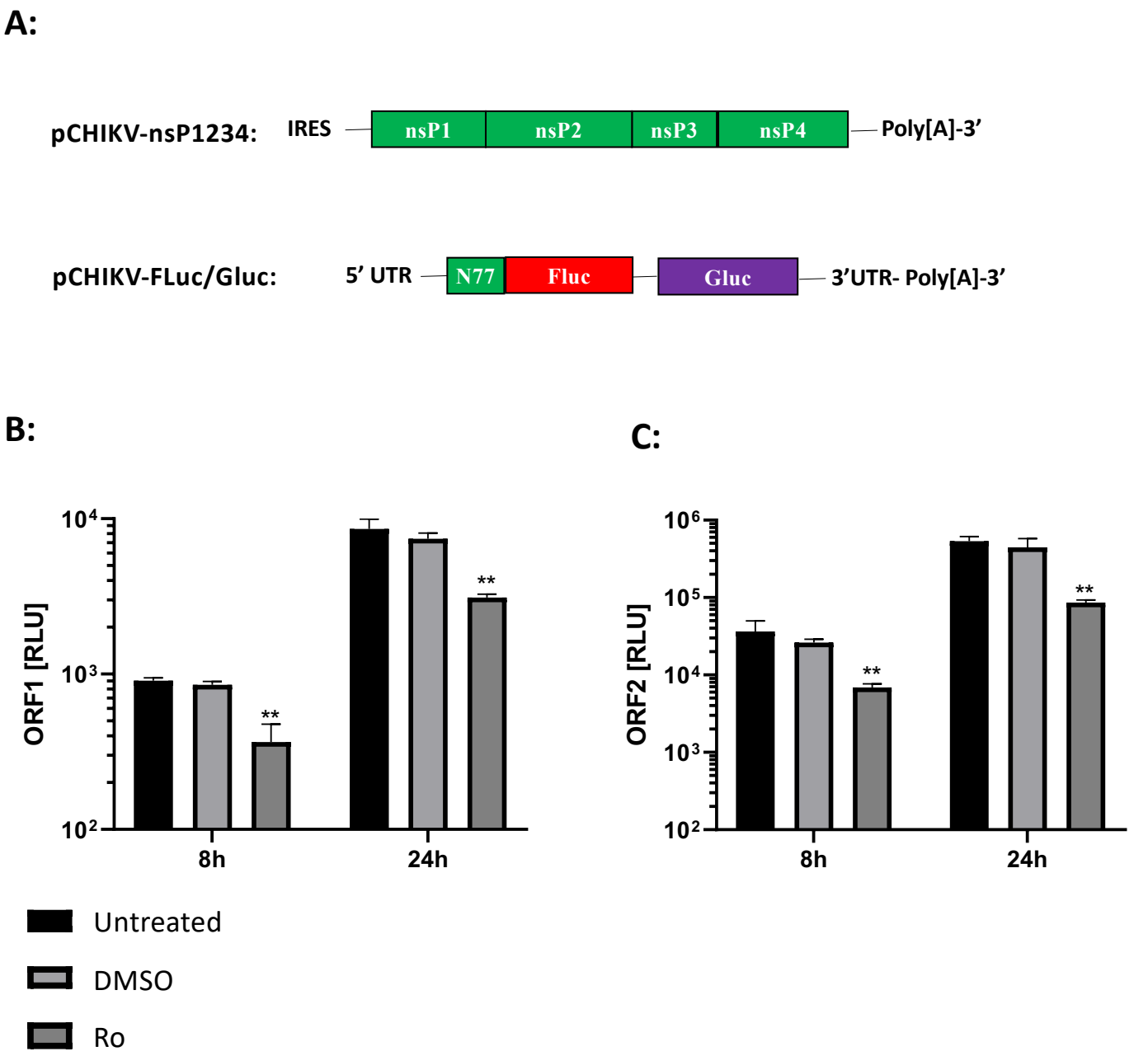

Figure 3. Ro signifyingly inhibits CHIKV genome replication. A) Schematic representation of CHIKV *trans*-complementation assay showing codon optimised pCHIKV-nsP1234 (top) from which the CHIKV nsPs were translated and pCHIK-Fluc/Gluc (bottom) in which ORF-1 was replaced by an Fluc reporter gene, fused to the first 77 nts or CHIKV ORF-1 (N77) down stream of the authentic CHIKV 5'UTR. ORF-2, flanked by the authentic intragenic (SG) and 3' UTRs, was replaced by a Gluc reporter gene. **B and C)** Ro significantly inhibited CHIKV genome replication of the *trans*-complementation assay, measured by both ORF-1 and ORF-2 expression, relative to DMSO treated negative controls at 8 and 24 hpt. N=3, error bars represent standard error from the mean and significance was measured by two-tailed T-test (* = $P < 0.05$, ** = $P < 0.01$, *** = $P < 0.001$).

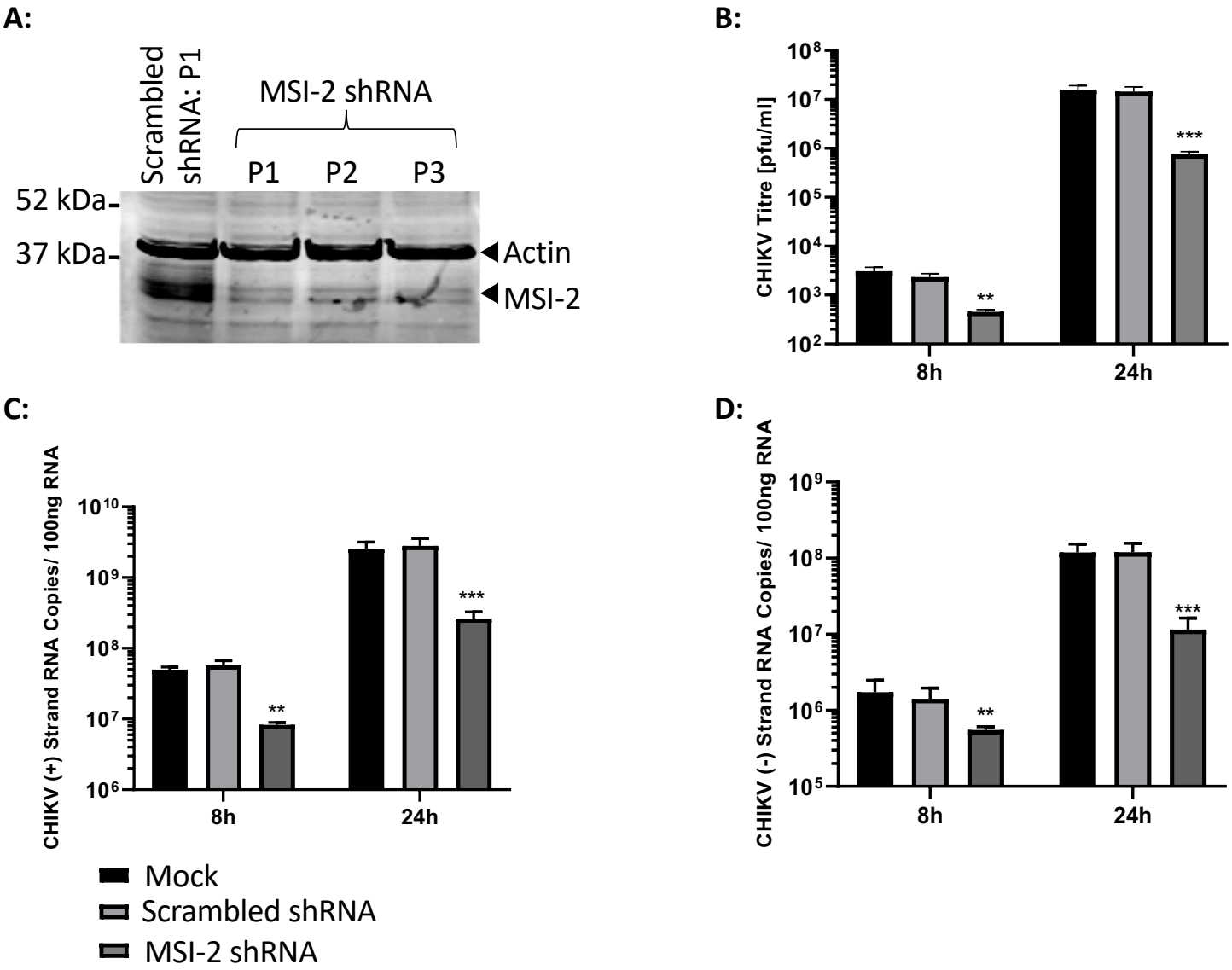

Figure 4. shRNA suppression of MSI-2 significantly inhibits replication of infectious CHIKV. A) Western blot analysis of total cellular protein extracted from Rd cells and compared to negative control scrambled shRNA, demonstrated consistent shRNA knockdown of MSI-2 over 3 serial passages (P1- P3). MSI-2 suppression significantly inhibited productive CHIKV replication, relative to scrambled shRNA at 8 and 24 hpi measured by plaque assay **(B)** and strand specific qRT-PCR for the the virus genomic **(C)** and negative intermediate **(D)** strands. N=3, error bars represent standard error from the mean and significance was measured by two-tailed T-test (* = $P < 0.05$, ** = $P < 0.01$, *** = $P < 0.001$).

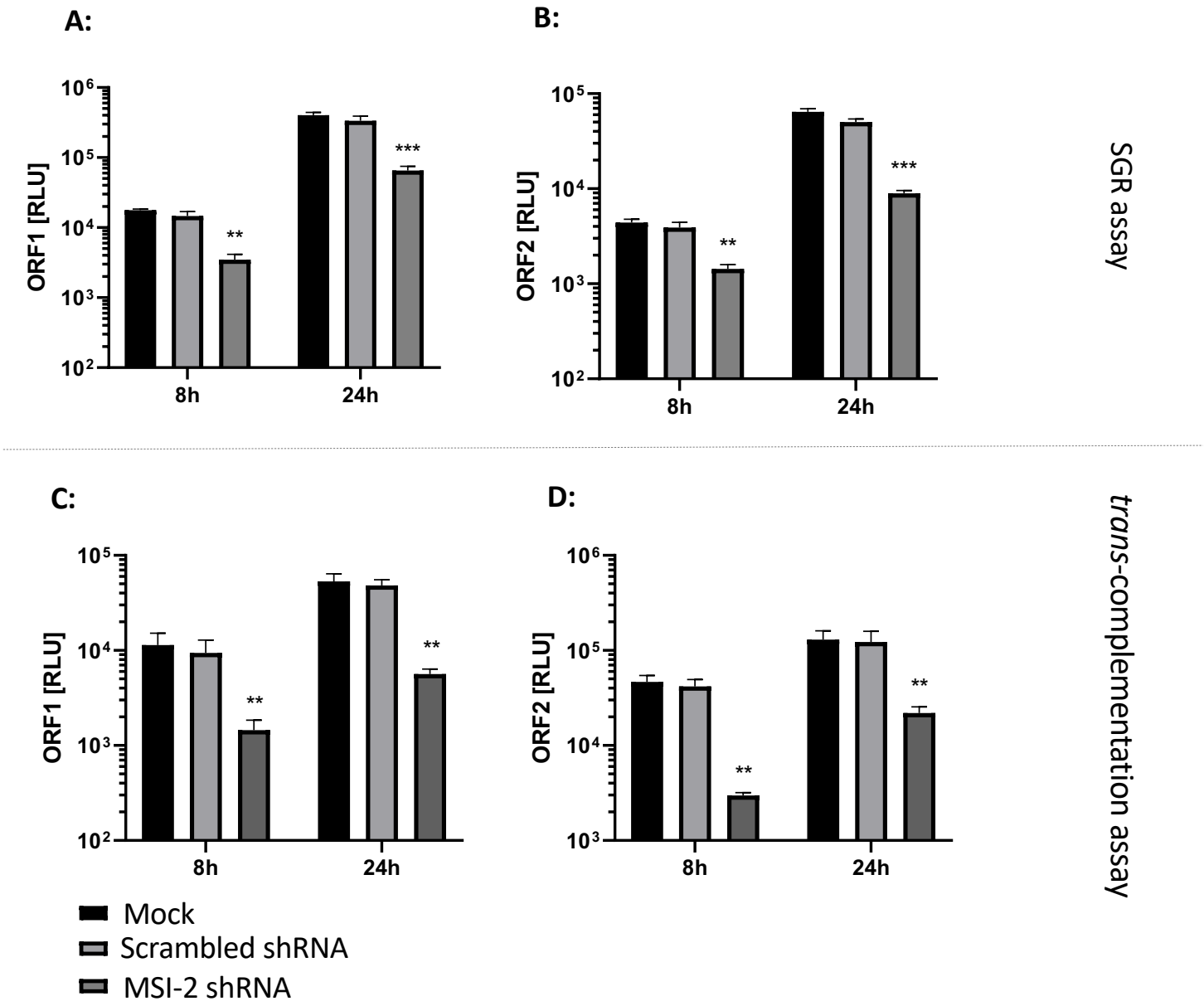

Figure 5. shRNA suppression of MSI-2 significantly inhibits CHIKV-SGR replication and CHIKV genome replication. A and **B)** shRNA suppression of MSI-2 significantly inhibited CHIKV-SGR replication, measured by both ORF-1 and ORF-2 expression, relative to scrambled shRNA negative controls at 8 and 24 hpt. **C** and **D**) shRNA suppression of MSI-2 significantly inhibited CHIKV genome replication of the *trans*-complementation assay, measured by both ORF-1 and ORF-2 expression, relative to DMSO treated negative controls at 8 and 24 hpt. N=3, error bars represent standard error from the mean and significance was measured by two-tailed T-test (* = $P < 0.05$, ** = $P < 0.01$, *** = $P < 0.001$).

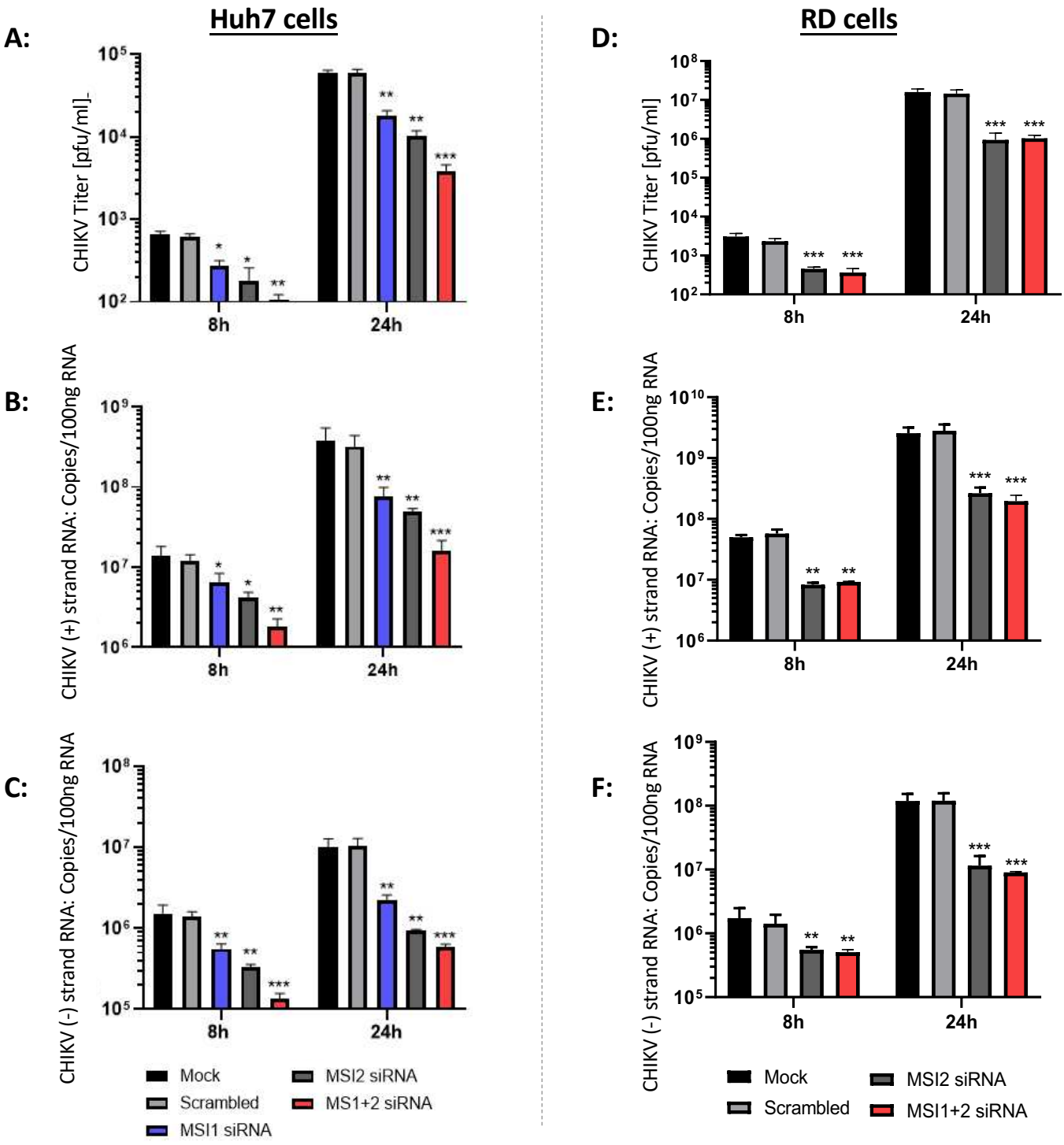

Figure 6: siRNA Depletion of either MSI-1 or MSI-2 significantly inhibited CHIKV replication in Huh7 cells and co-depletion of both MSI-1 and MSI-2 had a synergistic affect on CHIKV inhibition in Huh7 cells. siRNA depletion of MSI-2 significantly inhibited CHIKV replication in RD cells and co-depletion of both MSI-1 and MSI-2 did not increase the level of CHIKV inhibition. siRNA depletion of MSI-1 and MSI-2 significantly inhibited CHIKV replication in Huh7 cells relative to scrambled siRNA at 8 and 24 hpi measured by plaque assay **(A)** and strand specific qRT-PCR for the the virus genomic **(B)** and negative intermediate **(C)** strands. siRNA depletion of MSI-2 in RD cells significantly inhibited CHIKV replication in relative to scrambled siRNA at 8 and 24 hpi measured by plaque assay **(D)** and strand specific qRT-PCR for the the virus genomic **(E)** and negative intermediate **(F)** strands. N=3, error bars represent standard error from the mean and significance was measured by two-tailed T-test (* = $P < 0.05$, ** = $P < 0.01$, *** = $P < 0.001$).

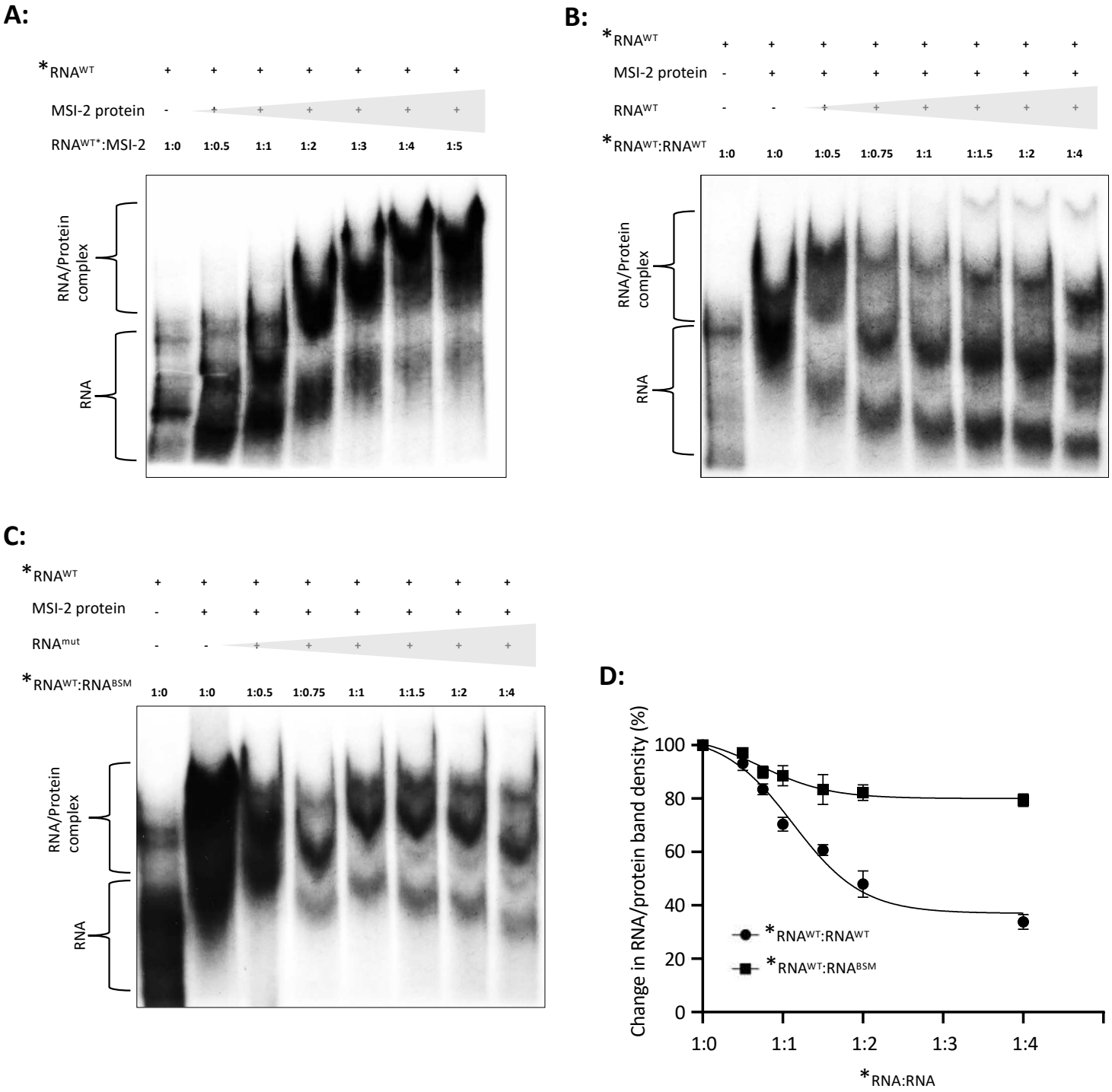

Figure 7. Native EMSAs between *in vitro* transcribed P^{32} 5' radiolabeled CHIKV RNA nts 1-330 (*RNA^{WT}) and recombinantly expressed MSI-2 demonstrated an RNA/protein interaction that was outcompeted by increasing concentrations of equivalent unlabeled (RNA^{WT}) but less efficiently by the same RNA incorporating BSM mutation $_{63}$AUUAAU$_{68}$ >$_{63}$CAACUU$_{68}$ (RNA^{BSM}). A) Increasing concentrations of MSI-2 intensified the observed band shift to the larger RNA/Protein complex and decreased the equivalent unbound RNA band. The interaction between a 1:4 ratio of *RNA^{WT}:MSI-2 was competed with increasing concentrations of unlabelled **B)** RNA^{WT} or **C)** RNA^{mut} ($_{63}$CAACUU$_{68}$-mut). **D)** Band shifts in the unlabeled RNA competition EMSAs were quantified by densitometry and expressed as % change in the density of the RNA/Protein complex bands, normalized to the equivalent total lane density, for each competition ratio and compared each time to ratio 1:0. N=3, error bars represent standard error from the mean and significance was measured by two-tailed T-test (* = P < 0.05, ** = P < 0.01, *** = P < 0.001). Grey block triangles indicate increasing concentrations of specific reactants.

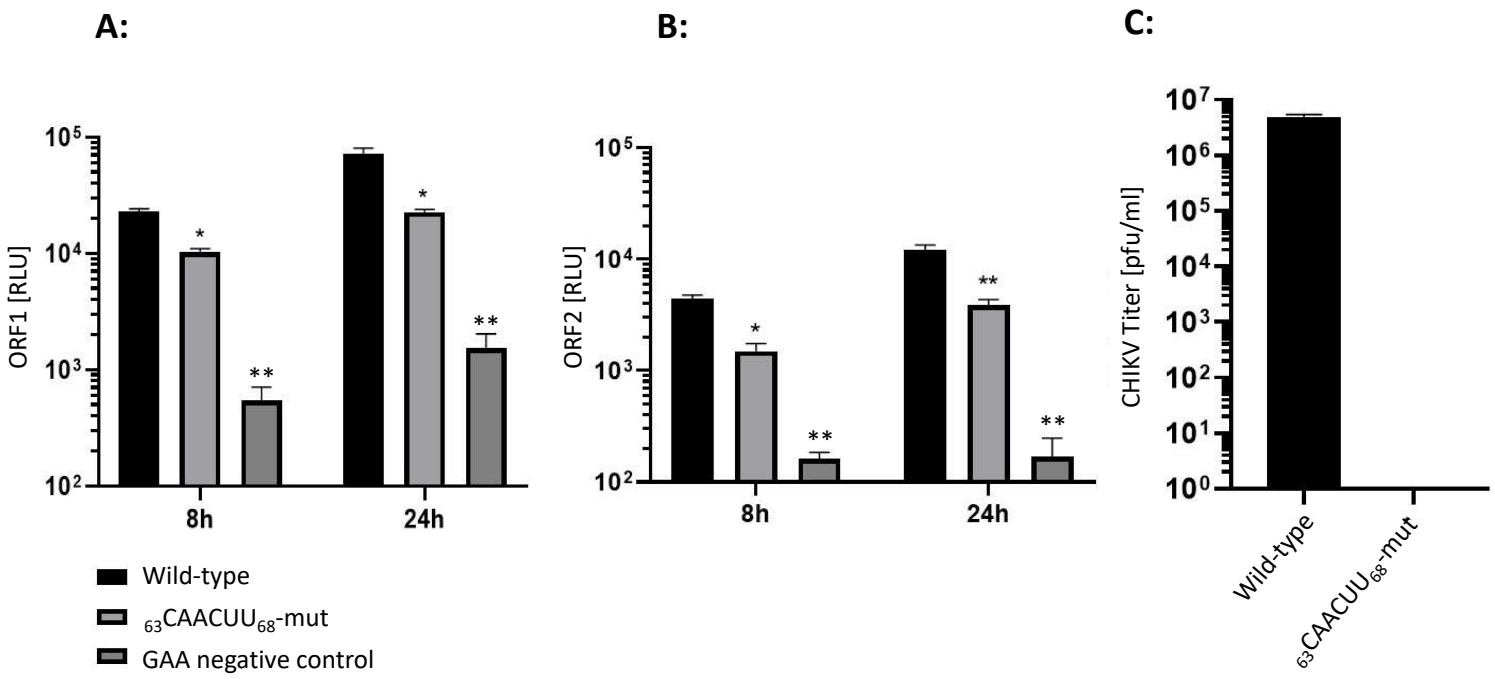

Figure 8. Substitutions within the predicted MSI binding site ($_{63}$CAACUU$_{68}$-mut) prevented rescue of BSM-mutant virus and significantly inhibited CHIKV genome replication. **A and B)** Mutation of the MSI binding site significantly inhibited CHIKV genome replication of the *trans*-complementation assay, measured by both ORF-1 and ORF-2 expression, relative to wild-type positive controls at 8 and 24 hpt. **C)** Mutation of the predicted MSI binding site prevented rescue of BSM-mutant CHIKV following transfection of capped *in vitro* transcribed RNA into BHK cells. Released virus was measured by plaque assay of supernatant 24 hpt and compared to positive control wild-type infectious CHIKV *in vitro* transcribed RNA, which was transfected and analysed in parallel. N=3, error bars represent standard error from the mean and significance was measured by two-tailed T-test (* = P < 0.05, ** = P < 0.01, *** = P < 0.001).

Supplementary data 1: Primers for the reverse transcription and quantitative PCRs for CHIKV strand-specific detection.

CIKV (-) strand detection	PCR	Primer sequence (5'-3')
CHIKV FT tag T	reverse transcription	GGC AGT ATC GTG AAT TCG ATG CGA CAC GGA GAC GCC AAC ATT
Tag T	quantitative	GGC AGT ATC GTG AAT TCG ATG C
CHIKV R T	quantitative	AAT AAA TCA TAA GTC TGC TCT CTG TCT ACA TGA
CHIKV (+) strand detection	PCR	Primer sequence (5'-3')
CHIKV RT tag T	reverse transcription	GGC AGT ATC GTG AAT TCG ATG CGT CTG CTC TCT GTC TAC ATG A
CHIKV F T	quantitative	AAT AAA TCA TAA GAC ACG GAG ACG CCA ACA TT
Tag T	quantitative	see above

Supplementary data 2: Expression and purification of MSI-2 Coomassie stained PAGE analysis following **A)** His Tag and **B)** Ion exchange chromatography. **C)** Ion exchange purified MSI-2 (8-193) analyzed by western blot, relative to total protein extracted from RD and Huh7 cells.

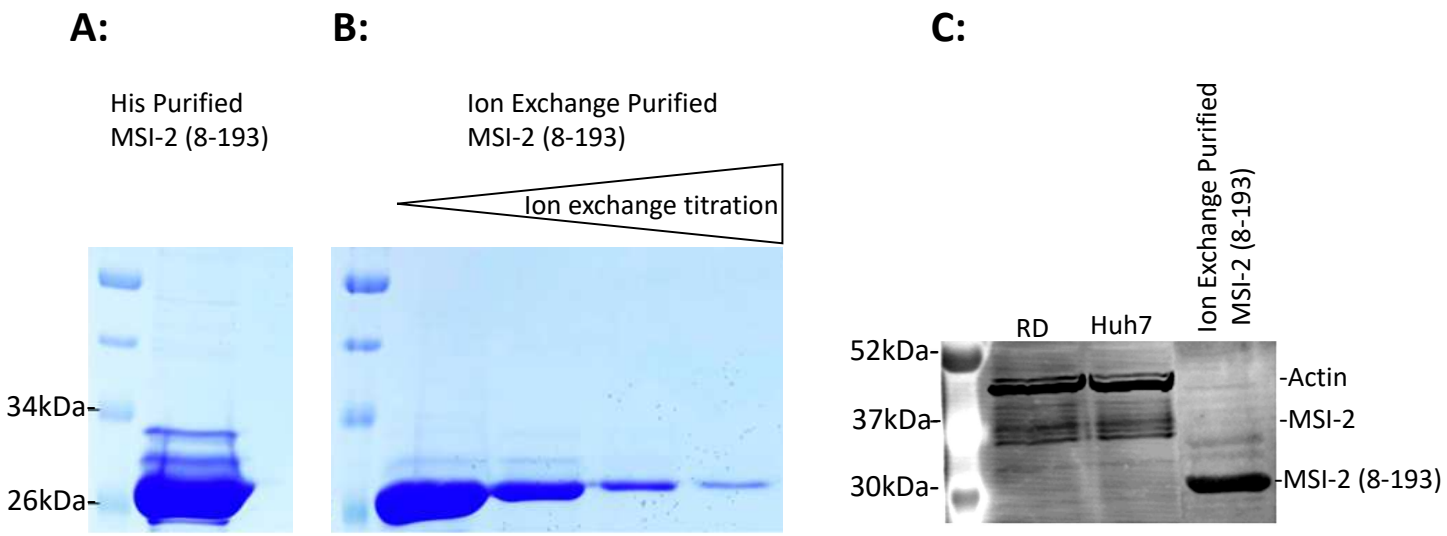

Supplementary data 3: MTT cytotoxicity assay for Ro 08-2750 in RD cells across a titration of 0, 05, 1, 3, 5 10 and 20uM. N=3, error bars represent standard error from the mean.

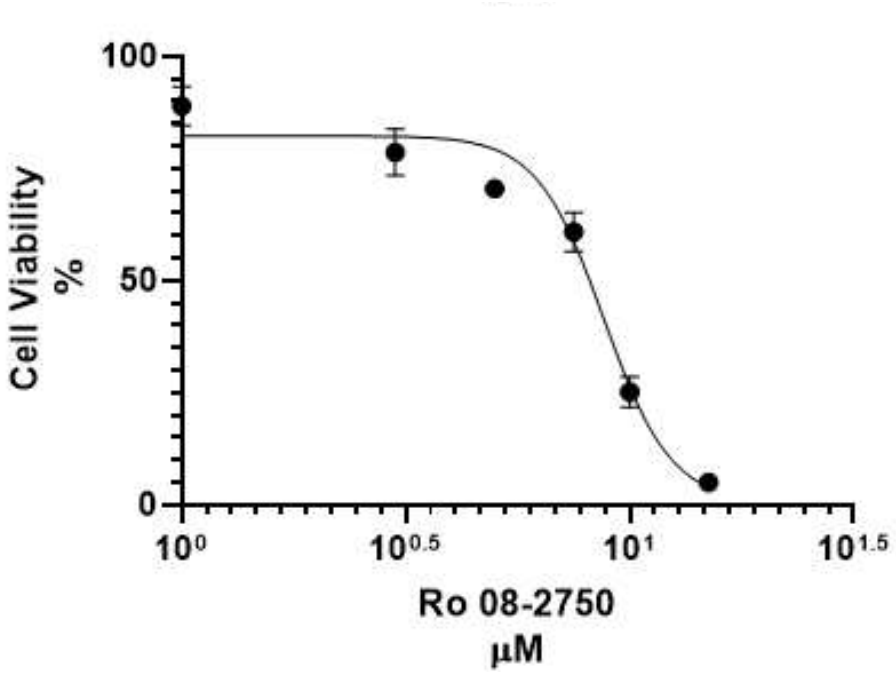

Supplementary data 4: A) MSI-1 and **B**) MSI-2 expression in RD and Huh7 cell lysate analyzed by western blot.

A)

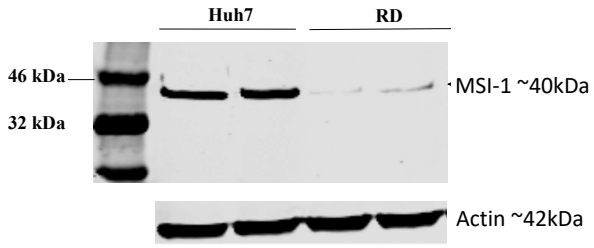

B)

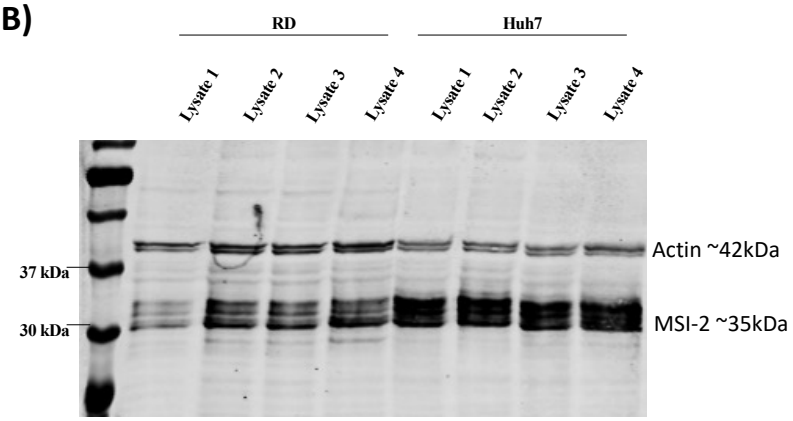
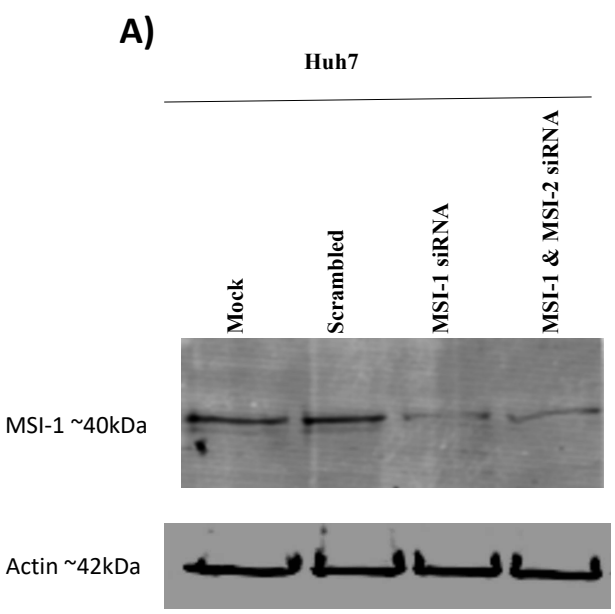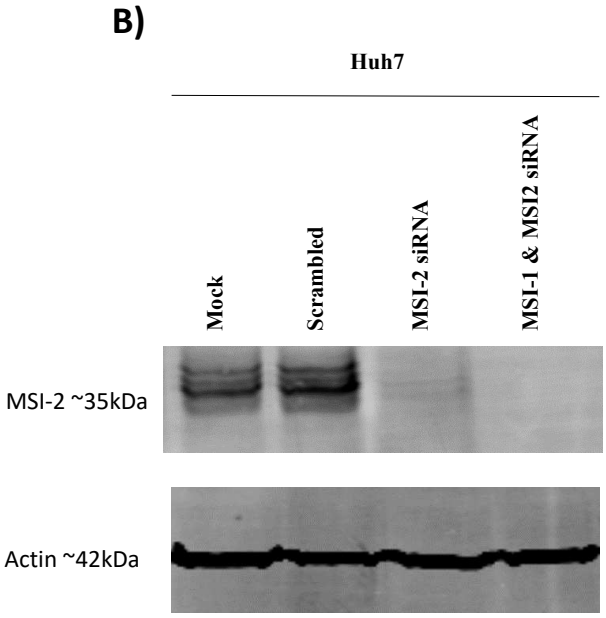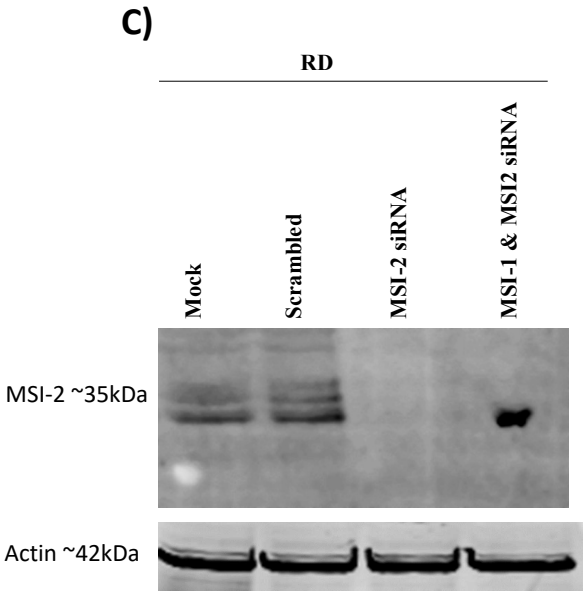
Supplementary data 5: Co-inhibition of MSI-2 and MSI-1 by siRNA in **A)** and **B)** Huh7 cells and **C)** RD cells